EXAMINATION OF akt AND foxo IN GROWTH AND SURVIVAL DURING CONDITIONS OF NUTRITIONAL STRESS IN Drosophila melanogaster

JENNIFER DENISE SLADE

Your file Votre référence
ISBN: 978-0-494-55267-4
Our file Notre référence
ISBN: 978-0-494-55267-4

Examination of *akt* and *foxo* in growth and survival during conditions of nutritional stress in *Drosophila melanogaster*

by

Jennifer Denise Slade

A thesis submitted to the School of Graduate Studies
in partial fulfillment of the requirements for the degree of
Masters of Science

Department of Biology
Memorial University of Newfoundland
April 16th, 2008
St. John's, Newfoundland and Labrador

Abstract

The insulin signaling pathway has been implicated as a regulator of cell growth and survival. To better understand the role of this pathway in these processes, two key effectors of insulin signaling, including the central component protein kinase akt, and its downstream target, the transcription factor foxo, were investigated. Novel derivatives of a P-element allele of *Drosophila melanogaster akt* exhibit lifespans which are comparable to controls. Analysis of somatic clones of the eye of these derivatives reveal that altered *akt* activity often leads to a reduction in cell number and size. Two *FRT/FLP* methods were used to generate clones, and the *ey-GAL4/UAS-FLP* method was shown to be more sensitive than the *ey-FLP* method. Analysis of *foxo* as a mediator of insulin signaling effects under various conditions of nutritional stress revealed its necessity during protein starvation, as *foxo* mutants did not live as long as controls or heterozygotes upon amino-acid starvation. A novel *foxo*-responsive luciferase assay revealed that as time of protein starvation increases, the expression of *foxo* is upregulated. Differences in total body mass between *foxo* mutants and controls after 96 hours of starvation suggest a possible maternal effect. Analysis of foxo protein activity within the akt^{04226} derivatives showed that both homozygous and heterozygous derivatives experienced a decrease in foxo activity compared to the control, but to varying degrees. Taken together, these findings support a role for insulin signaling in the control of cell growth and survival. In addition, they suggest the ability of insulin signaling to mediate cellular processes in response to nutrient availability.

Acknowledgements

I would like to express my sincere gratitude to my supervisor, Dr. Brian E. Staveley, for his advice, financial support and patience throughout the completion of my degree. I would also like to thank my committee Dr. Tom Chapman and Dr. Daniel MacPhee, and all of the members of Staveley lab for their advice and support. Thanks to Mr. Roy Ficken for help and use of his computer equipment, and to Mr. Peter Earle for assistance with computer applications. I would like to thank Ms. Lisa Lee for assistance with the scanning electron microscope. For assistance and access to equipment, I would like to thank Mr. Gary Collins and Mr. Craig Skinner. Funding for this work was provided by the Department of Biology and the School and Graduate Studies. Finally, I would also like to thank my family, friends for their encouragement, and my boyfriend, Keith Moore, for comforting me in stressful times and always believing in me.

Statement of Publication

Portions of the data presented within this thesis have been published, or submitted for publication, including some eye clone analysis, and the amino-acid starvation of the *foxo* mutants. The manuscripts accepted by *Drosophila Information Service* can be found in appendices A and B.

Table of Contents

List of Tables

List of Figures

List of Abbreviations

4EBP - eIF4E binding protein
AEL - after egg laying
AGC - protein kinase A/protein kinase G/protein kinase C
AH - after hatching
ASK1 - apoptosis signal regulating kinase 1
ATP - adenosine triphosphate
BAD - Bcl2 antagonist causing cell death
Bim - Bcl-2 interacting mediator of cell death
BSA - bovine serum albumin
CBP - CREB-binding protein
CCLR - cell culture lysis reagent
CDK - cyclin dependent kinase
CK1 - casein kinase 1
CNS - central nervous system
CREB - cAMP response element-binding protein
CyO - curly O
dakt - Drosophila akt
dfoxo - Drosophila foxo
dILP - Drosophila insulin-like peptide
dInR - Drosophila insulin receptor
DNA - deoxyribonucleic acid
dPTEN - Drosophila PTEN
dTOR - Drosophila TOR
DYRK1A - dual-specificity tyrosine-phosphorylated and regulated kinase 1A
e- ebony
eIF4E - eukaryotic initiation factor 4E
ey - eyeless promotor
FasL - Fas ligand
FKHR - forkhead in rabdomyosarcoma
FKHRL1 - FKHR-like 1
FLP - flippase
foxo - forkhead box, subgroup O
FRE - foxo recognition element
FRT - FLP recombination target
G6Pase - glucose-6-phosphatase
Gadd45 - G2 arrest and DNA damage repair gene 45
GLC - germline clone
GLUT1 - erythrocyte glucose transporter
GLUT4 - insulin-responsive glucose transporter
GSK3 - glycogen synthase kinase 3
GTP - guanine triphosphate
Hu - humeral
ICG - interval to cessation of growth

IGF - insulin-like growth factor
IGFR - IGF receptor
IIS - insulin/IGF signaling
InR - insulin receptor
IRS - insulin receptor substrate
JNK - jun N-terminal kinase
Ki - kinked
L - lobed
Luc - luciferase
MDM2 - mouse double minute 2
mfoxo - murine foxo
mnb - minibrain
MnSOD - manganese superoxide dismutase
mTOR - mammalian TOR
mTORC1/2 - mammalian TOR complex 1 and 2
NES - nuclear exportation sequence
NLS - nuclear localization sequence
PBS - phosphate buffered saline
PCD - programmed cell death
PDK1 - phosphoinositide-dependent kinase 1
PDK4 - pyruvate dehydrogenase kinase 4
PEPCK - phosphoenolpyruvate carboxykinase
PFK2 - phosphofructokinase 2
PGC-1 alpha - peroxisome proliferator-activated receptor (gamma) coactivator 1 (alpha)
PH - pleckstrin homology
PI3K - phosphotidylinositide 3-kinase
PIP2 - phosphotidylinositide 4,5-bisphophate
PIP3 - phosphotidylinositide 3,4,5-triphosphate
PTEN - phosphatase and tensin homologue
Rheb - Ras homologue enriched in brain
RLU - relative light units
RNA - ribonucleic acid
ROS - reactive oxygen species
RTK - receptor tyrosine kinase
S6K - ribosomal subunit 6-kinase
Sb - Stubble
SEM - scanning electron microscope
SGK - serum and glucocorticoid-regulated kinase
sir2 - silent information regulator 2
SIRT1 - silent information regulator of transcription 1
Tb - Tubby
TOR - target of rapamycin
TSC1/2 - tuberous sclerosis complex 1 and 2
UAS - upstream activation sequence
UV - ultraviolet

Introduction

Organs or tissues have a tendency to develop within a range of normal overall size, such that the cellular composition may vary from a large number of small cells, to a small number of large cells. Cell growth includes an increase in cell number and cell size, and while not mutually exclusive, both can be regulated by distinct extracellular processes (Coelho and Leevers 2000; Day and Lawrence 2000; Stocker and Hafen 2000; Johnston and Gallant 2002). A balance between the number and size of cells is important in development, and disruption of this balance may instigate the progression of disease. Examination of the processes that influence this balance is therefore beneficial to the understanding of the control of disease.

Mature *Drosophila melanogaster* normally develop over a period of 10 days. A sequence of three larval stages, separated by two moults, leads to a pupal stage. The larval stages are the essential feeding and growing stages, which last for five to six days until pupation. Several factors can influence the rate of growth during the larval stages such as nutrition, temperature, density of organisms present in the environment, and the underlying genetic mechanisms (Clancy et al. 2002; Kramer et al. 2003; Arking 2005; Geminard et al. 2006). Metamorphosis into the reproductively competent adult takes an additional four to five days. One crucial point in the control of growth in Drosophila is the achievement of the minimum weight required for transition from larvae to pupae, upon which any further feeding, or lack of feeding, will not affect this transition (Edgar 2006). This threshold is known as the critical weight. Drosophila larvae, when fed generously, can grow to, or past, the critical weight within four days. Restriction of dietary proteins slows this process, while total absence can halt growth altogether (Tatar

2007). Due to slowed growth, the larvae that reach the critical weight required to pupate develop into smaller adults. Once larvae have reached the critical weight required for pupation, they continue to feed for a period of time before undergoing the transition. This time is termed the interval to cessation of growth (ICG) (Edgar 2006). ICG length is likely influenced by temperature, changes in feeding behaviour or hormonal regulation in different environments. Once a mature adult Drosophila has eclosed, growth has ended (Mirth and Riddiford 2007). While the development and life cycle of insects may vary greatly from that of mammals, the mechanisms and genes which control growth appear to be very similar.

Growth depends largely upon nutrition. Nutrients circulating within the hemolymph via mobilization of triglycerides and glycogen stores allow cells to grow during times of nutritional stress (Edgar 2006). Often these energy stores are located in the fat body, an organ derived from mesoderm which functions in a manner analogous to that of the mammalian liver and adipose tissues. The fat body has been implicated as the nutrient sensing organ as it has been shown to produce growth factors in response to nutrition (Giannakou et al. 2004; Edgar 2006). Genetic manipulation of fat body metabolism is sufficient to reduce levels of insulin signaling in both larvae and adults.

In addition to cell growth, apoptosis or programmed cell death (PCD), is an important part of development. PCD can regulate cell number, control organ size, and eliminate superfluous structures and cells that are abnormal or exhausted (Greenwood and Gautier 2005; Twomey and McCarthy 2005). Developmental PCD occurs as either pre-determined autonomous cell death or non-autonomous cell death; the latter occurs due to lack of sufficient cell to cell interactions (Twomey and McCarthy 2005).

Autonomous cell death can be initiated either through underlying cell defects, such as DNA damage, or as a terminal differentiation fate. Non-autonomous PCD during development relies on cell to cell interactions and is required for the sculpturing of tissues or organs. Several cellular signals, including extracellular survival factors, cell surface death receptors, cell-lineage information, steroid hormones, and both intra- and extra-cellular stress signals, affect the non-autonomous initiation of PCD (Twomey and McCarthy 2005). The presence of both autonomous and non-autonomous types of developmental PCD in *Drosophila melanogaster* reinforces its use as an effective model to study apoptosis (Twomey and McCarthy 2005). Apoptosis is an essential process in the development of multicellular organisms, and acts to balance cellular proliferation.

One important cellular signaling pathway involved in the control of cellular growth and PCD is the insulin signaling pathway, which is highly conserved between invertebrates and mammals (Brogiolo et al. 2001). In Drosophila, the insulin signaling pathway has been shown to control cell size and growth, to regulate body size and nutrient usage (Coelho and Leevers 2000; Aoyama et al. 2006). When manipulated, several components of this pathway can affect growth rates of Drosophila. For example, when any of the seven Drosophila insulin-like peptide (dILP) genes are overexpressed, growth rates in larvae and adults are greatly increased, and ablation of the medial neurosecretory cells in the brain (the main producer of dILPs) leads to a decrease in the growth rate and final size (Edgar 2006). This suggests a role for insulin-like peptides, and thus the insulin signaling pathway, in growth control.

Insulin signaling

Insulin is a prominent peptide hormone in humans, and has been extensively studied due to its involvement in carbohydrate metabolism and progression of diseases such as diabetes. Insulin is a member of a peptide family that includes insulin-like peptides, and insulin-like growth factors (Garofalo 2002; Jackson 2006). In mammals, insulin is required for the conversion of glucose to glycogen, as well as the inhibition of glycogen breakdown and gluconeogenesis (Farese 2001). *Drosophila melanogaster* have seven insulin-like peptides and of these, dILP2 has been shown to interact with the Drosophila insulin receptor and is thought to be the most similar to human insulin (Brogolio et al. 2001; Edgar 2006). The insulin signaling pathway is associated with several functions including metabolism, cell size and proliferation, longevity and reproduction (Brogiolo et al. 2001; Barbieri et al. 2003; Cheng et al. 2005; Dionne et al. 2006), and is comprised of a number of components.

Insulin receptor signaling begins when the ligand binds to the insulin receptor. Insulin receptor substrates (IRS) and the phosphoinositide kinase-3 (PI3K) are recruited to the membrane. The synthesis of second messenger phosphoinositides by PI3K directs the kinase akt to the membrane, where it is activated to initiate the downstream effects of insulin signaling (Figure 1). Overexpression of the components of the pathway upstream of PI3K, including the dILPs, the insulin receptor (dInr) and the IRS (chico), in Drosophila results in larger than normal flies, while mutation or loss of function of these components results in size reduction and developmental delay (Wu and Brown 2006). A strong loss-of-function mutation in the insulin receptor results in an inability to produce

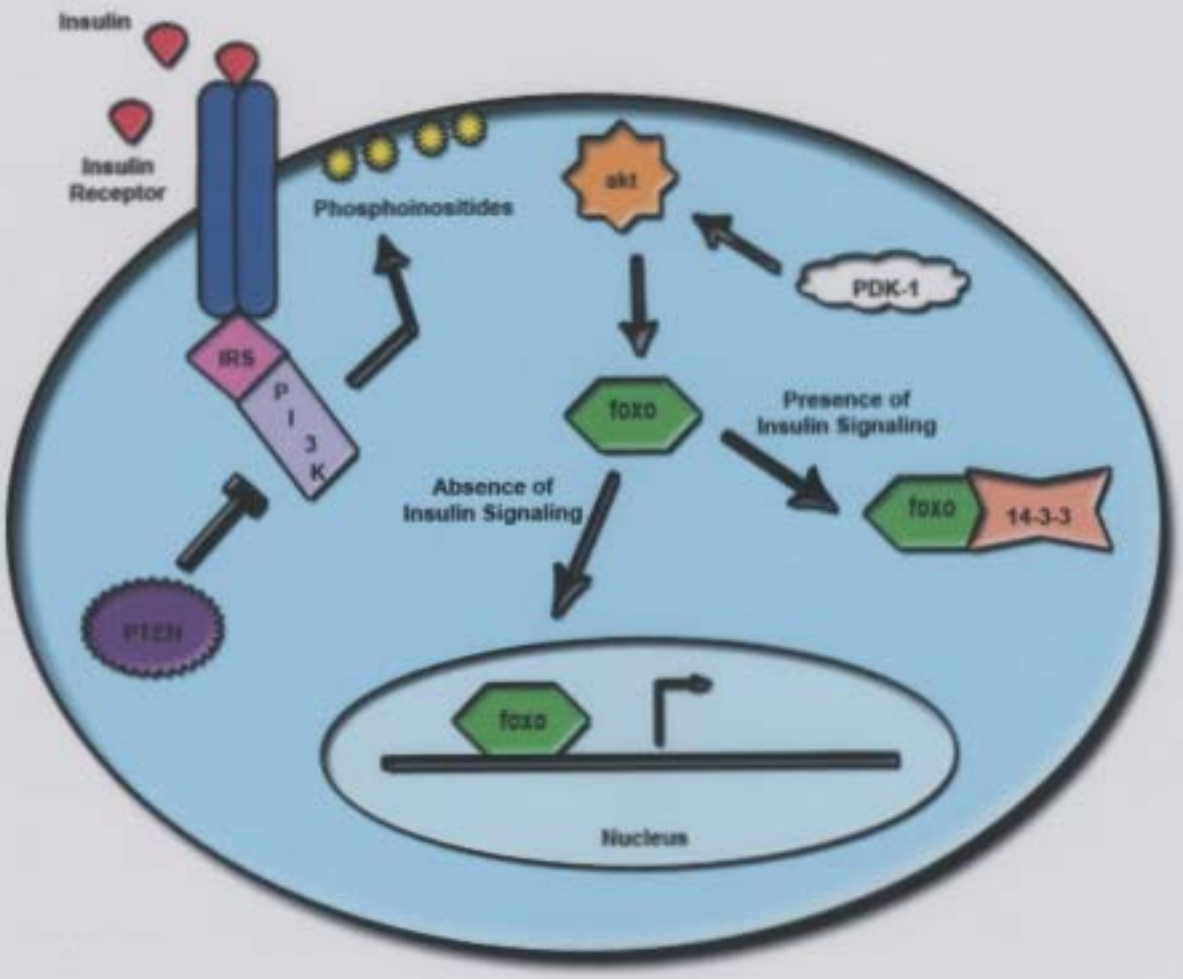

Figure 1: The akt kinase is central to the insulin signaling pathway. Insulin binds to the insulin receptor, leading to the recruitment of insulin receptor substrates and the kinase PI3K. PI3K produces phosphoinositides, which draws the kinase akt and PDK-1 to the membrane, where PDK-1 activates akt. In the presence of insulin signaling, akt leads to the inactivation of the foxo protein by phosphorylation, leading to the removal of foxo from the nucleus and its retention in the cytoplasm through the help of 14-3-3 proteins. In the absence of insulin signaling, foxo can enter the nucleus and enhance the transcription of its downstream targets. The PTEN protein acts to oppose insulin signaling through inhibition of PI3K.

adult flies, therefore the receptor is required for insulin signaling and survival (Poltilove et al. 2000; Whitehead et al. 2000). A negative regulator of the pathway, the phosphatase and tensin homologue (PTEN) gene functions to inhibit insulin signaling through the opposition of PI3K function. Overexpression of PTEN inhibits cell cycle progression and promotes apoptosis in the cells of the eye during its development (Goberdhan et al. 1999; Gao et al. 2000). This phenotype can be rescued by overexpression of functional PI3K and also, in some cases, the overexpression of dInr is able to rescue the phenotype (Wu and Brown 2006). This reinforces the role of insulin signaling in growth control.

Mutations in insulin signaling components affect the longevity of organisms (Gems and Partridge 2001; Bartke 2001; Cheng et al. 2005). This role for insulin signaling is tied to the control of cell size and growth as mutations in several of the pathway components, such as chico (Clancy et al. 2001), result in a reduced size of the overall organism and an extended lifespan. Downstream components of the pathway, including *akt* and *foxo*, have an impact on lifespan (Giannakou et al. 2004). The effects on cell growth and longevity obtained through altering components of insulin signaling resemble those that are seen through various nutritional stresses. Other potential functions for insulin signaling have not been fully explored. There have been associations between components of the insulin signaling pathway and neurogenesis that suggest a role for insulin signaling in the progression of several diseases (Leevers 2001; Lasko 2002; Goberdhan and Wilson 2003). The ability of insulin signaling to tie into many aspects of life makes it a central pathway to study diseases including, diabetes, cancer, and neurodegenerative disorders.

The kinase akt: a central component of insulin signaling

The kinase akt is a serine/threonine kinase belonging to the AGC (protein kinase A/protein kinase G/protein kinase C) class of kinases. Members of this family share the requirement of phosphorylation for activation (Scanga et al. 2000; Scheid 2000; Scheid and Woodgett 2001). Mammals possess three versions of *akt*, plus a closely-related kinase, serum and glucocorticoid activated kinase (SGK). Highly conserved homologues of mammalian *akt* exist in *Caenorhabditis elegans* and *Drosophila melanogaster* (Scheid and Woodgett 2001). Expression of *akt* in humans is widespread, and includes high concentrations in the brain, thymus, heart and lungs, and low expression levels in the kidney, liver and spleen (Scheid and Woodgett 2001). In Drosophila, *akt* is expressed throughout the organism during embryogenesis (Staveley et al. 1998; Scanga et al. 2000; Cavaliere et al. 2005). The high degree of protein conservation and the ubiquitous expression of the akt kinase highlights its importance.

The akt kinases share common structural characteristics including an N-terminal pleckstrin homology (PH) domain, a small region which connects the PH domain to serine/threonine specific kinase domain, and a C-terminal region essential for activity of the kinase domain (Scheid 2000; Scheid and Woodgett 2001). PH domains function in protein-lipid and/or protein-protein interactions, and this domain draws the akt protein to the lipid membrane when PI3K is activated via insulin signaling. The products that result from PI3K activation (phosphotidylinositols) show an affinity for PH domains, attracting akt, and other PH-domain containing kinases such as PDK-1 (phosphoinositide-dependent kinase 1). Once in close proximity, subsequent phosphorylation and activation of akt by PDK-1 can occur (Verdu et al. 1999; Toker and Newton 2000; Rintelen et al.

2001; Scheid and Woodgett 2001). Activation of akt *in vivo* requires phosphorylation at two residues: a threonine located in the activation loop, positioned near the catalytic core of the kinase domain, and a serine situated within the hydrophobic region near the C-terminus (Scheid and Woodgett 2001). Mutation of the central phosphoryated threonine residue to an alanine results in a 95% inhibition of activity; while mutation of only the carboxy-terminal serine residue to an alanine produces an 85% inhibition (Alessi and Cohen 1998). Thus, both sites are important to the activation of akt.

A role for *akt* in the control of cell growth and survival was discovered in experiments where *akt* expression was altered. Overexpression of *akt* in *Drosophila* leads to an increase in cell size, although there is no effect on cell growth rates or division. Underexpression or loss of *akt* can result in the production of smaller animals or, if severe enough, can be lethal (Kennedy et al. 1997; Staveley et al. 1998; Verdu et al. 1999). The role of *akt* in cellular survival was suggested by its inhibition of several pro-apoptotic genes (Kennedy et al. 1997; Nunez and del Peso 1998). As expected for a maternally expressed gene, *akt* female mutants are sterile, and Drosophila *akt* mutant germline clones undergo apoptosis (Staveley et al. 1998). This demonstrates that the activities of the akt kinase are of great importance to the survival of the cell, and to the overall organism.

The complexity of signaling downstream of akt kinase appears to be due to an array of targets and the varied biological processes that they control. Downstream targets of akt can be responsible for metabolic and cell growth functions, as well as cell survival, apoptosis and stress regulation. The akt kinase either inhibits or activates the downstream targets activity through direct phosphorylation (Scheid and Woodgett 2001;

Franke et al. 2003), which may lead to several outcomes. One outcome may be the alteration of the active site to prevent activation of its substrate (Cohen and Frame, 2001), or another may be a change in the binding affinity of the substrate for other proteins. As an example, akt can phosphorylate its substrate, causing that substrate to have a higher affinity for 14-3-3 proteins than those proteins with which it would normally react (Downward 2004). The 14-3-3 proteins are abundant in the cytoplasm, and therefore can bind with, and sequester, substrates in the cytoplasm.

Downstream targets of akt function in the regulation of cell survival and death. The apoptosis signal regulating kinase (ASK1) acts upstream of stress activated kinases, c-Jun N-terminal kinase (JNK) and p38 (Datta et al. 1999; Kim et al. 2001), which are directly linked to apoptosis. Overexpression of ASK1 can induce cell death in many types of cells (Alessi and Cohen 1998). However, when the *akt* gene is overexpressed, the ASK1 protein is phosphorylated and inactivated. By inhibiting ASK1, the downstream effectors JNK and p38 are inhibited (Kim et al. 2001). These represent a few examples of how the *akt* kinase exerts some of its control over cell survival.

In another aspect of anti-apoptotic control, the *akt* kinase phosphorylates the pro-apoptotic protein BAD which results in cell survival (Alessi and Cohen 1998; Scheid and Woodgett 2001). BAD is a Bcl-2 family member which, in its unphosphorylated state, will inhibit other Bcl-2 family members, such as Bcl-XL. The anti-apoptotic Bcl-XL protein maintains mitochondrial integrity by promoting transport of metabolites across the mitochondrial membrane and preserving cellular ATP production during periods with low levels of growth factors (Plas et al. 2001). BAD interacts with, and binds to, Bcl-XL to prevent it from protecting the cell. The akt kinase phosphorylates BAD in order to

increase its affinity for 14-3-3 proteins, thereby sequestering it in the cytoplasm, and rendering it inactive. Thus, when BAD is phosphorylated by akt, it cannot bind to Bcl-XL, which allows Bcl-XL to protect the cell from apoptosis by blocking the release of cytochrome c from mitochondria. In a similar manner, the akt kinase functions to inhibit the activity of the transcription factor foxo.

The transcription factor foxo: an important downstream target of akt

The *foxo* gene encodes a transcription factor containing a 110 amino acid DNA binding domain, termed the forkhead domain. A large number of structurally related genes compose a family of forkhead proteins (Lee and Frasch 2004) which are classified into subclasses from foxa through to foxq. The subclass *foxo* (forkhead box group O) proteins have been identified in several organisms, including *Caenorhabditis elegans*, zebrafish, Drosophila, mouse, rat and humans (Lee and Frasch 2004). The *foxo* group is comprised of the proteins foxo1, foxo3A and foxo4 in humans, foxo in Drosophila, and daf-16 in the nematode *C. elegans*. The highly conserved nature of this protein alludes to its importance.

The foxo transcription factors are negatively regulated via exclusion from the nucleus to prevent activation of their downstream targets (Burgering and Medema 2003; Puig et al. 2003; Barthel et al. 2005; Puig and Tjian 2005). There are several intramolecular domains which play a part in the shuttling of foxo from the nucleus to the cytoplasm. Phosphorylation is the major event that results in the relocation of foxo proteins, and is initiated through different pathways, one being the PI3K/*akt* pathway (Van Der Heide et al. 2004). Once activated, akt can relocate from the plasma membrane

throughout the cytoplasm and nucleus to phosphorylate foxo within the forkhead domain, and at either end of the protein (Van Der Heide et al. 2004). Phosphorylation at the N-terminus and in the forkhead domain has been shown to be necessary for foxo translocation, as these regions are associated with the nuclear localization sequence (NLS) and the area of the protein involved in 14-3-3 protein binding (Van Der Heide et al. 2004; Perrot and Rechler 2005). A nuclear localization sequence (NLS) is essential to keeping a protein within the nucleus, while a nuclear exportation sequence (NES) is required to keep a protein in the cytosol. The foxo proteins contain both types of sequences and, therefore, can be shuttled in and out of both subcellular compartments.

Four sequential steps comprise the translocation of foxo from the nucleus into the cytoplasm. The first step is phosphorylation of the akt site within the forkhead domain and disrupting the NLS function. One of the residues which akt phosphorylates is located within the NLS, and upon phosphorylation, the NLS area of the protein is altered so that it becomes non-functional, promoting foxo translocation to the cytoplasm. The second step involves phosphorylation of the other akt sites, located at either end of the protein. This leads to a string of phosphorylated serines at the C-terminal end, which may become further phosphorylated by other kinases such casein-kinase-1 (CK1) and dual-specificity regulated kinase-1A (DYRK1A). The third step involves the highly phosphorylated foxo stimulating a high affinity for foxo proteins and 14-3-3 binding proteins. Lastly, the phosphorylated foxo forms a complex with adaptor proteins, leading to its export from the nucleus (Van Der Heide et al. 2004). Disrupting any one of these steps is sufficient to halt nuclear export and cause foxo to build up within the nucleus (Van Der Heide et al. 2004). Thus, each step may be considered to be of equal importance.

In addition to the control of foxo translocation in and out of the nucleus, there are two other mechanisms by which foxo activity can be regulated. First, as it can be proteolytically cleaved, alteration of its stability can be regulated (Huang et al. 2004; Van Der Heide et al. 2004). Secondly, the efficacy of foxo can be controlled through regulation of its transcriptional activity (Van Der Heide et al. 2004; Vogt et al. 2005). This can be carried out through modulation of its DNA binding efficiency, association of foxo proteins with various co-factors, and through acetylation and deacytelation of the foxo transcription factor itself (Van Der Heide et al. 2004; van der Horst et al. 2004). Modification of the DNA binding ability of foxo proteins is linked to the phosphorylation of the *akt* site located within the forkhead domain. Mutation of this serine to an alanine is sufficient to disrupt DNA binding (Van Der Heide et al. 2004). The mechanisms which control the translocation, cleavage or transcriptional activation of foxo activity can regulate the balance between *foxo*'s influence upon downstream targets that control apoptosis and those that control the cell cycle.

As foxo is regulated by a series of components belonging to a number of signaling pathways, it often mediates transcriptional regulation of these pathways. As such, it controls a number of downstream targets involved in several important cellular functions. These include control of metabolism, cell cycle regulation, DNA repair, apoptosis and protection against oxidative stress (Burgering and Kops 2002; Barthel et al. 2005; Puig and Tjian 2005; Gershman et al 2007). Through these many functions, the transcription factor foxo can affect cell growth and survival.

Downstream targets involved in the control of cell growth include those which affect metabolism, such as phosphoenolpyruvate carboxykinase (PEPCK), the Drosophila

insulin receptor, and the Drosophila eukaryotic initiation factor 4E-binding protein (d4EBP), among many others. In mammals, PEPCK is one of the rate-limiting liver enzymes responsible for the control of hepatic gluoneogenesis. The gene that encodes PEPCK is upregulated or downregulated in response to certain hormones, such as insulin, when they are secreted in response to various nutrient conditions (Aoyama et al. 2006; Matsumoto et al. 2006). When *foxo* is upregulated, so is 4EBP, which binds to the messenger RNA 5' cap-binding protein eIF4E and regulates its activity. While the complete biological role of 4EBP is still unknown, it has been shown to be important in times of nutritional and oxidative stress in Drosophila (Miron et al. 2001). In *foxo*-null mutants, overexpression of 4EBP can rescue adult flies from severe oxidative stress (Miron et al. 2001), and is therefore an essential downstream target of *foxo* under these conditions.

The foxo protein also affects cell growth through regulating insulin signaling via negative feedback. In the absence of insulin, akt is not activated and foxo remains within the nucleus where it can enhance the transcription of its downstream targets. One of these targets is the insulin receptor. During times of nutritional stress, *foxo*, followed by the transcription of the insulin receptor, is upregulated, so that cells become more sensitive to insulin signaling, aiding in a quick response once access to nutrition is restored. Once this happens, akt is activated, exporting foxo from the nucleus causing downregulation of the transcription of the receptor (Puig et al. 2003; Hwangbo et al. 2004). This demonstrates that foxo is an important endpoint of insulin signaling.

Finally, foxo can regulate cell growth through downstream targets which affect the cell cycle, such as $p27^{kip1}$ and several of the cyclin proteins. In humans, $p27^{kip1}$

inhibits cyclin-dependant kinases (cdks) (Dijkers et al. 2000), which aid in promoting the transitions between cell-cycle phases through the phosphorylation of a plethora of substrates. Specifically, $p27^{kip1}$ binds to Cdk2 and inhibits its activity. Overexpression of $p27^{kip1}$ in human cells leads to cell-cycle arrest in the G1 phase, which has also been observed when *foxo*, and thus $p27^{kip1}$, is upregulated (Dijkers et al. 2000; Van Der Heide et al. 2004). The activity of *foxo* therefore plays a role in the control of cell cycle progression.

In addition to regulating cell growth, the transcription factor foxo can play a large role regulating cell survival by protecting the cell from oxidative stress through downstream targets such as manganese superoxide dismutase (MnSOD) and the growth-arrest and DNA damage response protein 45 (Gadd45) (Van der Heide et al. 2004; Furukawa-Hibi et al. 2005). Superoxide dismutase functions to protect redox sensitive cellular machinery from damage through catalyzing the conversion of the superoxide anion into oxygen and hydrogen peroxide (Essers et al. 2004; Culotta et al. 2006). Gadd45 works to repair the damage to DNA and proteins that occurs upon exposure to environmental stress, and all members of the Gadd45 family are expressed in response to stress stimuli that induce DNA damage (Tran et al. 2002). When *foxo* is active in the nucleus, it may upregulate the transcription of MnSOD and Gadd45 to aid in DNA repair and removal of superoxide anions to help cells deal with oxidative stress.

Regulation of cell survival by foxo is also carried out through downstream targets which contribute to apoptosis, or programmed cell death. Apoptosis plays a central role during the development of multicellular organisms, and in the progression of many diseases. A downstream target of foxo which is involved in the control of apoptosis is

the Fas ligand (FasL). This extracellular ligand binds to the Fas receptor, which is a death receptor (Vermeulen et al. 2005; Yan and Shi 2005). Death receptors, when bound with a ligand, recruit adaptor proteins, that then act as the link between ligand-receptor and the activation of downstream effectors of PCD, known as caspases. These caspases are important for the degradation of cellular and nuclear proteins, leading to the destruction of the cell (Vermeulen et al. 2005; Yan and Shi 2005). The expression of *foxo* can play an important role in the initiation of PCD.

In summary, the transcription factor foxo is regulated through a series of different proteins, in a variety of manners, and its activity can affect the regulation of a number of downstream targets. The complexity of foxo signaling allows this protein to partake in the control of intricate processes such as cell growth and survival, and therefore makes foxo activity valuable during various challenging conditions, such as nutritional stress.

Starvation and foxo in flies

As an organism eats and digests, it converts food intake into a storable form, often glycogen and fat. In Drosophila, the organ which stores energy is the fat body (Giannakou et al. 2004). During the lifetime of most organisms there is a fluctuation in the availability of nutrition. When there is limited nutrient uptake, glycogen is catabolized and used for energy. In order to deal with situations of low nutrient availability, complex signaling cascades are required, such as the insulin pathway. This pathway appears to work through blending both nutrient uptake and control of cell growth during development via the action of its downstream targets, such as foxo.

When growing Drosophila larvae are starved of nutrients, development halts, and is resumed when nutrients are returned (Britton et al. 2002; Kramer et al. 2003). When larvae are raised under nutrient limited conditions, the adults are smaller than those eclosing from well-fed larvae, a phenotype similar to that observed in flies with an inhibition of insulin signaling (Kramer et al. 2003). When insulin signaling is inhibited through an overexpression of PTEN or dominant negative versions of PI3K, developmental arrest similar to that seen during starvation in first instar larvae occurs (Britton et al. 2002). Overexpression of *foxo*, such as its activation in the absence of insulin signaling, results in the same phenotypes which arise when larvae are starved (Kramer et al. 2003). A reduced insulin signaling level is required for maximal survival during starvation, as overexpression of insulin signaling components, such as PI3K or dInr, leads to the inability of Drosophila to survive during nutritional stress (Britton et al. 2002). In addition, the expression of Drosophila insulin-like peptides (dILPs) is regulated by the availability of nutrients, and overexpression of these results in larger animals (Brogiolo et al. 2001). These findings suggest that insulin signaling is involved in mediating the developmental response of larvae to starvation, and leads to the conclusion that in the absence of adequate nutrition, insulin signaling is reduced, allowing foxo to enhance the transcription of downstream targets to aid in the overall survival of the organism.

Previous studies of *foxo*'s role during nutritional stress, by inducing ubiquitous expression of *foxo* in the first instar larvae, caused a complete arrest of growth, yet the larvae survived for several days (Kramer et al. 2003; Junger et al. 2003). Analysis of endogenous *foxo* activity and *foxo* loss-of-function demonstrated a role of *foxo* in the

organism's response to amino acid starvation. Newly hatched Drosophila larvae require nutrients in order to increase their body mass via replication of cells in mitotic tissues. In contrast, when larvae are hatched into conditions of amino acid starvation, they live in a state of developmental arrest until nutrients become available (Beadle et al. 1938). Loss of *foxo* resulted in an inreased sensitivity to starvation due to low levels of amino acids (Junger et al. 2003). When measuring the amount of foxo present in various nutrient conditions, it has been shown that when nutrient levels are low, *foxo* expression is increased. Upon return of nutrients, *foxo* levels return to basal levels (Kramer et al. 2003). Ectopic expression of Drosophila *foxo* leads to inhibition of growth and generation of small adults. In addition, when there is an excess of foxo activity in larvae, feeding behaviour is altered. This highlights the importance of *foxo* in times of nutritional stress, and taken together, these results show the importance of insulin signaling and *foxo* in the survival of organisms during nutritional stress.

Experimental rationale

The main goal of this research was to gain a better understanding of the role of insulin signaling in cell growth, survival and during conditions of nutritional stress. To do this, a subset of *akt* P-element derivatives were analyzed to understand the impact of akt kinase activity on the control of cell growth and survival. In addition, activity of an *akt* downstream target, the transcription factor foxo, was examined under conditions of nutritional stress because of foxo's critical role in activation of several stress response genes. The development and use of a novel technique, a *foxo*-responsive luciferase assay was implemented in the study of these insulin signaling components.

Materials and Methods

Drosophila media and culture

Stocks and crosses were maintained on a standard medium containing cornmeal, molasses, yeast, agar and water. Fresh food was prepared by Dr. Brian E. Staveley approximately twice a month and was treated with propionic acid and methylparaben to prevent growth of mold. Seven milliliter aliquots of media was poured into vials, allowed to solidify, and refrigerated at 4 to 6°C. Stocks were maintained on solid media for two to three weeks before transfer onto new media to reculture. Stocks were kept at room temperature (22 ± 2°C) while crosses and experiments were carried out at 25°C.

Drosophila control stocks

The control line w^{1118} was received from Dr. Howard Lipshitz (University of Toronto), and the control line w^{1118}; FRT^{2A} FRT^{82B} akt^{+} was derived from lines obtained from Norbert Perrimon, Harvard University. Wild-type *OrR* stock was obtained from the Bloomington Drosophila Stock Center.

Derivative lines generated from a P-element allele of akt

The initial P-element insertion line akt^{04226} was obtained from the Bloomington Drosophila Stock Center. This line contains a P-element inserted within the 5' untranslated region of the *akt* gene on the third chromosome. The novel derivatives of akt^{04226} were generated by Dr. Brian E. Staveley. The P-element insertion line was crossed to a line containing a stable source of transposase, $P\Delta 2\text{-}3$, ry^{+} (Robertson et al. 1988). The offspring of the dysgenic males and *Ly/TM3, Sb ry* females were selected for

loss of the P-element by the eye colour gene *rosy*. Two hundred *ry* revertants were created. To allow for clonal analysis, recombinants of FRT^{2A} FRT^{82B} and the novel derivatives of akt^{04226} were generated and maintained (Staveley, unpublished). A subset of these recombinants were selected for analysis (Table 1). Although sequencing of these derivatives is not yet complete, it is expected that they differ from the wild-type akt^{+} line by either a small section of the P-element remaining within the control region, or by a loss of a small section of the control region upon removal of the P-element.

Longevity of akt^{04226} derivative heterozygotes

Slight alterations in the activity of *akt* may lead to an increase in longevity, similar to that which has been observed with mutants of the other components of the insulin signaling pathway, including the IRS chico (Clancy et al. 2001). Preliminary analysis of the akt^{04226} derivative lines revealed a slight extension in lifespan among heterozygotes having one wild-type allele and one allele derived from akt^{04226} (Slade 2005). To re-examine this, another longevity experiment was conducted. From the lines akt^{PR44}, akt^{PR57}, akt^{PR76}, *and* akt^{PR87}, adult heterozygous virgin females were mated to heterozygous males. Several single vial matings of three to five females plus two males were made of each genotype which were transferred onto new food every two days. A cohort of adult heterozygous male flies (example genotype $akt^{PR44}/+$) were collected upon eclosion. Approximately one hundred fifty or more flies were aged per genotype, at a density of ≤ 20 flies per vial. Adults were kept on fresh media which was replenished every four to six days. Flies were observed and scored every two days for presence of deceased adults. Flies were considered dead when they did not display movement upon

agitation. Longevity data was analyzed using the GraphPad Prism 4.02 program. Survival curves were compared using the log-rank test, a statistical test that compares the actual and expected number of failures (death) between survival curves at each individual failure event. Significance was determined at 95%, at a P-value less than or equal to 0.05.

Clonal analysis of akt^{04226} derivatives

Mosaic eye clones were created via the yeast site-specific recombination FLP/FRT system and examined to analyze the effect of derivative alleles upon eye growth, cell survival and development. This system depends upon the presence of FRT sites near the centromere of the 3R chromosome that bears the *akt* gene, and tissue-specific expression of the enzyme FLP (Theodosiou and Xu 1998). FLP was driven by the *eyeless* promoter that directs expression in the developing eye tissue. In the presence of FLP, homologous chromosomes undergo mitotic recombination between the FRT sites located on chromosome pairs. Heterozygous parent cells can produce both homozygous akt^{04226} derivative cells containing two copies of the derivative allele, and wild-type cells containing two copies of wild-type akt^{+}. In this system, the akt^{+} daughter cells are lost due to the presence of a recessive cell lethal mutation located on the same arm of the chromosome bearing the akt^{+} allele. Thus, in the eyes of clone bearing flies, the surviving cells bear two copies of the akt^{04226} derivative allele under investigation. This procedure is effective for the study of a homozygous phenotype in a heterozygous background; and is necessary when the homozygous phenotype is lethal or developmentally delayed, as is the case with a number of *akt* mutants.

Table 1: Full genotypes of control and akt^{04226} derivative stocks implemented in experiments and abbreviations used to refer to each stock throughout the thesis.

Full Genotype	***Abbreviation***
Controls	
w^{1118}	w^{1118}; akt^{+}
w^{1118}; $FRT^{2A}FRT^{82B}$ akt^{+}	w^{1118}; FRT akt^{+}
w^{1118}; akt^{+}/akt^{+} *(Product of outcross between* w^{1118} *and OrR)*	$w^{1118;}$ akt^{+}
P-element insertion line *(Berkeley Drosophila Stock Center)*	
w^{1118}; $FRT^{2A}FRT^{82B}$ akt^{04226}	akt^{04226}
Derivatives of akt^{04226} *(Staveley, unpublished)*	
w^{1118}; FRT^{2A} FRT^{82B} akt^{PR10}/*TM6B, Hu Tb e*	akt^{PR10}
w^{1118}; FRT^{2A} FRT^{82B} akt^{PR12} /*TM6B, Hu Tb e*	akt^{PR12}
w^{1118}; FRT^{2A} FRT^{82B} akt^{PR19}/*TM6B, Hu Tb e*	akt^{PR19}
w^{1118}; FRT^{2A} FRT^{82B} akt^{PR24}/*TM6B, Hu Tb e*	akt^{PR24}
w^{1118}; FRT^{2A} FRT^{82B} akt^{PR44}/*TM6B, Hu Tb e*	akt^{PR44}
w^{1118}; FRT^{2A} FRT^{82B} akt^{PR52}/*TM6B, Hu Tb e*	akt^{PR52}
w^{1118}; FRT^{2A} FRT^{82B} akt^{PR57}/*TM6B, Hu Tb e*	akt^{PR57}
w^{1118}; FRT^{2A} FRT^{82B} akt^{PR60}/*TM6B, Hu Tb e*	akt^{PR60}
w^{1118}; FRT^{2A} FRT^{82B} akt^{PR62}/*TM6B, Hu Tb e*	akt^{PR62}
w^{1118}; FRT^{2A} FRT^{82B} akt^{PR76}/*TM6B, Hu Tb e*	akt^{PR76}
w^{1118}; FRT^{2A} FRT^{82B} akt^{PR87}/*TM6B, Hu Tb e*	akt^{PR87}
w^{1118}; FRT^{2A} FRT^{82B} akt^{PR174}/*TM3, Sb*	akt^{PR174}
w^{1118}; FRT^{2A} FRT^{82B} akt^{PR195}/*TM3, Sb*	akt^{PR195}

The *akt*^{04226} derivative stocks contain FRT sites near the centromere of the 3R chromosome arm containing *akt*. The full genotype of these lines are *w; +/+; P[FRT ;w*$^{+}$*]*^{2A} *P[ry*$^{+}$ *neo*^{R} *FRT]*^{82B} *akt*^{PR**}*/TM6B or TM3,* where ** represents the allele of *akt* derived from *akt*^{04226}. Males of these lines were crossed to females possessing *eyeless-FLP*, the FRT at the base of 3R, and a distal recessive lethal allele. The full genotypes of Drosophila stocks containing *eyeless-FLP* are *y*^{d2} *w*^{1118}*; P14*^{2}*, P{GMR-lacZ.C(38.1)}*^{TPN1}*; P{ry*$^{+t7.2}$*=neoFRT}*^{82B}*, P{w*$^{+t*}$ *ry*$^{+t*}$*=white-un1}*^{90E}*, l(3)cl-R3*^{1}*/TM6B, P{y*$^{+t7.7}$ *ry* $^{+t7.2}$*=Car20y}*^{TPN1}*, Tb*^{1} for method one (Newsome et al. 200) and is hereby designated the "*ey-FLP*" method. The genotype *y w; P{w*$^{+m}$*=GAL4-ey.H}*$^{3-8}$*, P{w*$^{+mC}$*=UAS-FLP1.D}*^{JD1}*; P{ry*$^{+t7.2}$*=neoFRT}*^{82B}*, P{w*$^{+mC}$*=GMR-hid}*^{SS4}*, l(3)CL-R*^{1}*/TM2* was the line used for method two, hereby termed the "*ey-GAL4/UAS-FLP*" method (Stowers and Schwarz 1999). Five sets each of three to five virgin females plus two males were incubated on fresh food and left for 48 hours. These sets were transferred to fresh food every 2 days. Adult males of the desired phenotype (lacking *Ubx* for *TM2* or Tb and *Hu* for *TM6B* markers) were collected at the same time of day and aged for three days. Flies were then flash frozen at –70°C before preparation for scanning electron microscopy. Preparation included mounting upon aluminum SEM studs, dessication and sputter coating in gold. Three to five images of each genotype were taken on a Hitachi S-570 SEM at 150X magnification and analyzed using NIH Image J software (Abramoff et al. 2004).

The foxo mutant stocks

The *foxo* mutant alleles $foxo^{21}$ and $foxo^{25}$ were obtained from Martin Junger and Ernst Hafen of the University of Zurich. Both of these alleles contain a premature stop codon near the beginning of the *foxo* gene resulting in complete loss of the protein (Junger et al. 2003). These alleles were created through EMS mutagenesis, therefore transhomozygotes ($foxo^{21}/foxo^{25}$) were created to study the null phenotype and avoid any second site lethality, as described by the discoverers. The *foxo* mutant chromosomes were balanced over the *TM6C, Tb* balancer chromosome containing the *Tubby* (Tb) marker to aid in selection of specific larval genotypes.

Longevity of foxo mutant adults on starvation media

To obtain adult *foxo* heterozygous and transhomozygous mutants, *w;* $foxo^{21}/TM6C$ and *w;* $foxo^{25}/TM6C$ flies were crossed together, and to w^{1118} flies. From these reciprocal crosses, males of the desired phenotype were collected within 24 hours of eclosion. One hundred fifty or more flies were collected per genotype, and maintained in non-crowded conditions by a maximum number of 20 flies per vial. Adults were aged on fresh amino-acid starvation medium, consisting of 5% sucrose in PBS and agar, and was replenished every four to six days. Studies of survival upon the starvation media was carried out and analyzed as described previously for the longevity of the akt^{04226} derivatives. Flies were scored every two days for presence of deceased adults. Adults were considered dead when they did not display movement upon agitation. Results were analyzed using the GraphPad Prism 4.02 program. Survival curves were compared using the log-rank test. This is a test statistic that compares the actual and expected number of

Table 2: Genotypes of *foxo* mutants and *foxo*-responsive luciferase stocks used in experiments and abbreviations.

Full Genotype	***Abbreviations***
foxo lines (Junger and Hafen)	
w; foxo^{21}/TM6C	*foxo^{21}*
w; foxo^{25}/TM6C	*foxo^{25}*
foxo-responsive luciferase lines (Kramer 2005)	
w; FRE-luc$^{4.2}$/CyO	*FRE-luc$^{4.2}$*
w; FRE-luc$^{5.5}$/CyO	*FRE-luc$^{5.5}$*
w; FRE-luc$^{4.2}$/CyO; foxo^{21}/TM6C	*FRE-luc$^{4.2}$, foxo^{21}*
w; FRE-luc$^{4.2}$/CyO; foxo^{25}/TM6C	*FRE-luc$^{4.2}$, foxo^{25}*
w; FRE-luc$^{5.5}$/CyO; foxo^{21}/TM6C	*FRE-luc$^{5.5}$, foxo^{21}*
w; FRE-luc$^{5.5}$/CyO; foxo^{25}/TM6C	*FRE-luc$^{5.5}$, foxo^{25}*

failures (death) between survival curves at each individual failure event. Significance was determined at 95%, at a P-value less than or equal to 0.05.

Determination of weight differences of foxo mutants under conditions of nutritional stress

To determine the effects of starvation on the weight of adults, male adult *foxo* mutants were collected as in the longevity on starvation media experiment described on page 23. As males eclosed, they were placed on either fresh food or starvation media and left for 96 hours. After this time, males were flash frozen at –70°C and then immediately weighed. A minimum of 20 flies per genotype for each condition (fed or starved) was weighed. Graph was created using GraphPad Prism 4.02 program. Statistical analysis was performed as standard error of the mean and columns were compared using a paired t-test statistic.

The foxo-response element luciferase (FRE-luc) reporter transgene

FRE-Luc flies were created using the *8xFK1tkLuc* construct provided by William Biggs III (Biggs et al. 1999) which contains the firefly luciferase gene under the control of a herpes simplex virus thymidine kinase minimal promoter and eight direct repeats of a *foxo*1 enhancer sequence, which is referred to here as the *foxo* response element (FRE) (Figure 2). Firefly luciferase is a 61 kDa monomer that catalyzes the mono-oxygenation of beetle luciferin, a relatively stable molecule found only in luminous beetles (which include fireflies). This enzyme works by using ATP as a cofactor to oxidize its substrate, luciferin, into oxiluciferin (Wood et al. 1989). A by-product of this reaction is light. This light, referred to as bioluminescence, is a type of chemiluminescence as it is

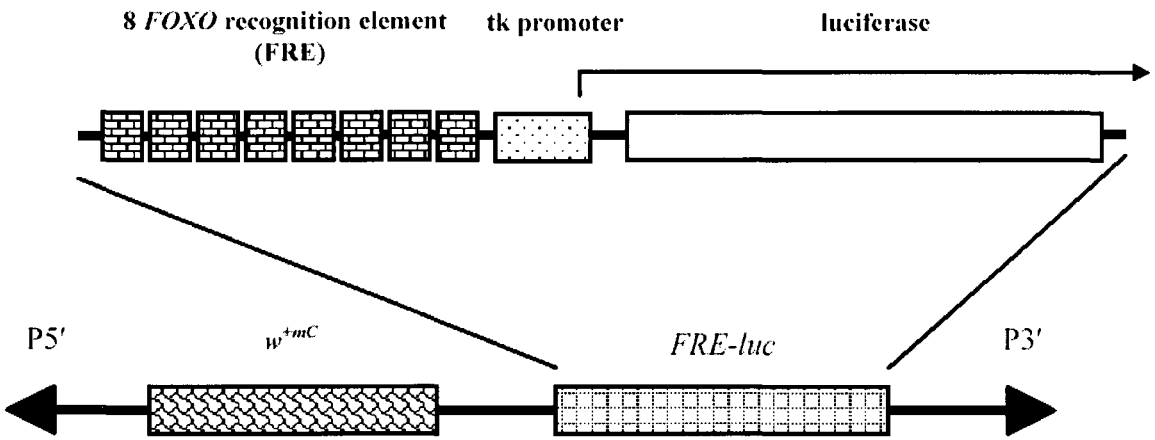

Figure 2: Schematic representation of the FRE-luc transgene
Eight direct repeats of the *foxo* recognition element (FRE) are located upstream of a minimal herpes simplex thymidine kinase (tk) promoter fused to the *luciferase* gene. This was inserted into the multiple cloning site of the *pP{CaSpeR-1}* transformation vector (Slade et al. 2005; Kramer, Slade and Staveley, submitted).

formed through a chemical reaction. The transgene allows the expression of the luciferase gene when *foxo* is expressed (Biggs et al. 1999). This construct was cloned into the *pP(CaSpeR-1)* transformation vector and injected into the developing germ line of *white*$^{-/-}$ embryos (Slade et al. 2005; Kramer, Slade and Staveley, submitted). Transgenic flies were identified based on red eye colour. A stable insertion was isolated on the second chromosome.

Analysis of foxo activity using luciferase assays

Luciferase assays were performed to evaluate *foxo* activity during times of nutritional stress. Collection of larvae included several crosses. To obtain control adults, a line which was homozygous for the *FRE-luc* transgene on the second chromosome was crossed to a w^{1118} line to produce offspring of the genotype *w; FRE-luc*$^{4.2}$*/+; +/+*. Mutant heterozygotes were obtained through the crossing of *FRE-luc*$^{4.2}$ homozygous flies to *foxo*^{21} or *foxo*^{25} flies, and to obtain transhomozygotes with one copy of the reporter gene, flies with the genotype *w; FRE-luc*$^{4.2}$*/FRE-luc*$^{4.2}$*; foxo*$^{21\ or\ 25}$*/TM6C* were crossed to appropriate *foxo* heterozygotes with the reporter gene.

To expediate collection of larvae, crosses were set up on apple juice plates (50% apple juice and 3% agar) and allowed to lay eggs for 20 hours. Each morning, plates were cleared of any larvae which hatched overnight. 6 hours after the initial clearing, all larvae were collected and placed on plates of standard media (cornmeal, molasses, yeast and agar). The larval progeny were selected for analysis based on the altered body shape resulting from the *Tb* marker. As it is difficult to distinguish between *Tb* and non-*Tb* larvae in the first instar, genotypes were selected at 48 hours after hatching (AH). After 48 hours, larvae had grown to a sufficient degree to enable phenotyping. Larvae of the

correct phenotype were collected and placed into plates containing starvation media. This media was 20% sucrose in PBS. Larvae were collected and frozen at –70°C at 0 hours and 48 hours from the initiation of starvation.

Protein extraction

Adults or larvae were collected in triplicate groups of ten and then flash frozen at -70°C for a minimum of 5 minutes. Protein extraction was performed according to the Promega Luciferase Assay System manual (Promega Corporation, Madison, Wisconsin). Flies or larvae were placed in 200 µl of cell culture lysis buffer, and homogenized by grinding in a 1.5 ml microcentrifuge tube. Samples were then subjected to a freeze-thaw cycle three times, that included flash freezing the samples in ethanol at -70°C, and thawing the samples in a 37°C water bath. The tubes were centrifuged at 10,000 rpm for 15 minutes to remove cellular debris. The supernatant was collected in a fresh tube. The procedure of homogenization, freezing and thawing, centrifugation and collection of supernatant was repeated on the pellet fraction, with the second supernatant pooled with the original.

Determination of protein concentration

Protein amounts were quantified using the *DC* Protein Assay kit from Bio-Rad (Bio-Rad Laboratories, Hercules, California). Protein concentrations of extracts were determined against a standard curve of BSA concentrations and using manufacturer's instructions. Working reagent A, an alkaline copper tartrate solution, and reagent B, a dilute Folin reagent, are required for protein quantification. The proteins and copper react

in the alkaline medium, and this leads to the reduction of Folin and colour production. 33 µl of each protein sample was added to a clean, dry cuvette. 167 µl of reagent A and 1.3 mL of reagent B were added to each protein sample. The cuvette was gently agitated to mix reagents and samples. After 15 minutes, the absorbance of each cuvette was read at 750 nm by a Genesys 10 spectrophotometer from Thermo Electron Corporation.

Quantification of luciferase expression

To quantify the luciferase activity present in each protein sample, 20 µl of sample plus 100 µl of Steady Glo reagent (Promega Luciferase Assay System) were added to wells in a dark 96-well plate. The plate was placed into the luminometer Top Count NXT microplate scintillation and luminescence counter. Amounts of luciferase activity was then quantified and compared to control samples.

Analysis of luciferase activity data

Luciferase data was analyzed using GraphPad Prism 4.02. The absorbance of each sample was calculated and compared to the slope of BSA standards to determine the amount of protein. The relative light unit (RLU) of each sample in comparison to the amount of protein was determined by dividing the average light absorption (from the luminometer) of each sample by 0.02 mL, the amount of sample used. This gives the RLU/mL. This was then divided by the protein concentration of each sample to give RLU/mg protein. The RLU/mg protein was then graphed for each sample. Standard error of the mean was calculated from multiple measurements.

Building foxo-responsive luciferase/akt^{04226} derivative lines

To generate the *foxo*-responsive luciferase lines, *akt*^{04226} derivative alleles were crossed to a double balancing line of the genotype: *w*^{1118}; *L/CyO; Ki ftz/TM6B, Hu Tb e*. This involved the collection of virgin females of the *akt*^{04226} derivative lines and mating in a vial of fresh food with males from the balancer line (Figure 3). Males were selected from these generated lines based on the presence of *CyO* (a curled wing) and absence of *Ki*, a phenotype that displays a "kinked" bristle, and crossed to female virgins of *foxo*-responsive luciferase lines (genotype: *w*^{1118}; *FRE-luc*$^{4.2}$*/CyO, Ki ftz/TM6B, Hu Tb e* or *w*^{1118}; *FRE-luc*$^{5.5}$*/CyO, Ki ftz/TM6B, Hu Tb e*) to obtain the *foxo*-responsive luciferase lines (Table 3). To confirm a stable line of *foxo*-responsive luciferase/*akt*^{04226} derivative genotype, both virgin females and males with the phenotypes curly wings (*CyO*) and *Humeral* were crossed.

Analysis of foxo activity in akt^{04226} *derivative alleles*

Luciferase assays were performed to determine the effect of altering *akt* activity upon *foxo*. The protocol for the luciferase assay can be found above as *Protein extraction, Determination of protein concentration, Quantification of luciferase expression* and *Analysis of luciferase activity data* on pages 28 and 29.

Collection of *akt*^{04226} derivatives for assays was achieved by preparing crosses of virgin females and males of the genotype *w; luc*$^{5.5}$ */CyO; akt****/TM6B* or *TM3* where akt** represents each of the *akt*^{04226} derivatives balanced over either *TM6B* or *TM3*. Crosses were maintained at 25°C. The *akt*^{04226} derivative homozygotes (males and females) were collected every day for two weeks. The luciferase 5.5 lines produced both

Table 3: Full genotypes and abbreviations for *foxo*-responsive luciferase/akt^{04226} derivative lines created.

Full Genotype	***Abbreviation***
w^{1118}; *FRE-luc***/CyO; akt+/ TM6B, Hu Tb e*	*FRE-luc*$^{+}$*/CyO; akt+*
w^{1118}; *FRE-luc***/CyO;* akt^{04226}*/ TM6B, Hu Tb e*	*FRE-luc***/CyO;* akt^{04226}
w^{1118}; *FRE-luc***/CyO;* akt^{PR10}*/ TM6B, Hu Tb e*	*FRE-luc*/CyO;* akt^{PR10}
w^{1118}; *FRE-luc*/CyO;* akt^{PR12}*/ TM6B, Hu Tb e*	*FRE-luc*/CyO;* akt^{PR12}
w^{1118}; *FRE-luc*/CyO;* akt^{PR19}*/ TM6B, Hu Tb e*	*FRE-luc*/CyO;* akt^{PR19}
w^{1118}; *FRE-luc*/CyO;* akt^{PR24}*/ TM6B, Hu Tb e*	*FRE-luc*/CyO;* akt^{PR24}
w^{1118}; *FRE-luc***/CyO;* akt^{PR44}*/ TM6B, Hu Tb e*	*FRE-luc*/CyO;* akt^{PR44}
w^{1118}; *FRE-luc***/CyO;* akt^{PR52}*/ TM6B, Hu Tb e*	*FRE-luc*/CyO;* akt^{PR52}
w^{1118}; *FRE-luc***/CyO;* akt^{PR57}*/ TM6B, Hu Tb e*	*FRE-luc*/CyO;* akt^{PR57}
w^{1118}; *FRE-luc***/CyO;* akt^{PR62}*/ TM6B, Hu Tb e*	*FRE-luc*/CyO;* akt^{PR62}
w^{1118}; *FRE-luc***/CyO;* akt^{PR76}*/ TM6B, Hu Tb e*	*FRE-luc*/CyO;* akt^{PR76}
w^{1118}; *FRE-luc***/CyO;* akt^{PR87}*/ TM6B, Hu Tb e*	*FRE-luc*/CyO;* akt^{PR87}
w^{1118}; *FRE-luc***/CyO;* akt^{PR174}*/ TM6B, Hu Tb e*	*FRE-luc*/CyO;* akt^{PR174}
w^{1118}; *FRE-luc***/CyO;* akt^{PR195}*/ TM6B, Hu Tb e*	*FRE-luc*/CyO;* akt^{PR195}

*: indicates two luciferase transgene lines, 4.2 or 5.5

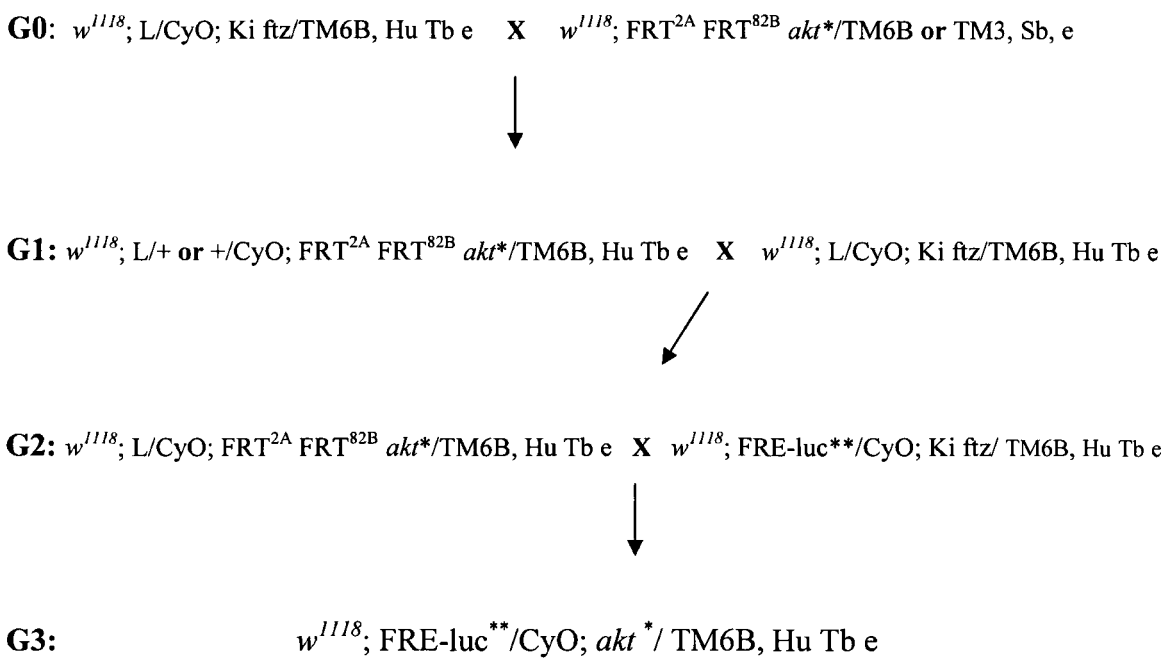

Figure 3: Schematic of crosses made to obtain *foxo*-responsive luciferase/*akt* lines. Note that all balancer chromosomes TM6B carry the marker genes Hu, Tb and e. * indicates the line of *akt* used in the cross, whereas ** indicates the type of *FRE-luc* used in the cross.

heterozygous and homozygous adults in sufficient quantity and were thus chosen as the version to analyze. The luciferase 4.2 version of the lines were not used in analysis. Flies were flash frozen and stored at -70°C until assays were performed, as described above.

Results

The akt^{04226} allele and its derivatives

The P-element insertion allele of the *akt* gene, akt^{04226}, was identified in a large-scale gene disruption project carried out by the Berkeley Drosophila Genome Project (Perrimon et al. 1996; Spradling et al. 1999). This allele has been described as semilethal, with homozygous individuals having reduced body and cell size (Perrimon et al. 1996; Gao et al. 2000). Derivatives of this allele, produced through imprecise excision, have subtle phenotypes (Slade 2005). Preliminary examination of several of these lines included analysis of the developmental timing from egg laying to eclosion, longevity and cell growth in the eye. Many of these derivatives exhibited a delay in development from 1 to 3 days. Longevity analysis determined that homozygous derivatives exhibit decreased lifespan to varying degrees, while heterozygotes demonstrate variable survival curves compared to wild-type controls. Lastly, biometric analysis demonstrated that the eye of the derivatives were smaller primarily due to a smaller cell size. Cell number varied among derivatives, with some being greater than controls. These preliminary findings provided the basis for the experiments that follow.

Lifespan of akt^{04226} derivative heterozygotes does not differ from controls

Analysis of the longevity of akt^{04226} derivatives indicated that selected heterozygotes could be placed into three arbitrary groups, including those with a lifespan similar to the control, those with a reduction in lifespan compared to the control, and those with an extension in lifespan when compared to the control (Slade 2005). The median lifespan for heterozygotes in the extended lifespan group fell between days 64 and 70. Compared to the control median lifespan of 60 days, each was significantly

different with P-values all less than 0.0001. As this result seemed to be noteworthy, we conducted the experiment again to determine if these results were reproducible.

To investigate extended lifespan phenotypes in the derivative lines, a number of controls were examined (Figure 4A). One was the original w^{1118} ; akt^{+} laboratory stock (blue line). The second and third controls were also of the genotype w^{1118}; akt^{+}, but were generated by different means. The second control consisted of males from a stock originally generated from crossing w^{1118} to *OrR* (purple line), and the third control consisted of first generation males from the cross of w^{1118} to *OrR* (pink line). Analysis of the lifespan of controls provided the standard to which the heterozygotes could be compared. The original w^{1118};akt^{+} stock control (blue line) had a median survival of 48 days and 0% survival by day 64, which was the lowest survival rate overall. The mixed generation control line of w^{1118}; akt^{+} (purple line) experienced a survival trend with median survival at day 54 and extinction by day 74. The first generation control line of w^{1118}; akt^{+} (pink line) had a median survival at day 64 and extinction at day 78. This control had a greater survival rate by 10 days, likely due to lack of accumulated deleterious modifiers, and was established as the baseline to which to compare the derivatives.

The survival rates of the heterozygous derivatives fell below the selected w^{1118}, akt^{+} controls (Figure 4B). The median lifespan for the derivatives ranged between days 56 and 64, while maximum lifespan of the selected heterozygous derivatives fell between days 74 and 80. The survival trends for the derivatives akt^{PR44}, akt^{PR76} and akt^{PR87} are not significantly different from the control. The longevity of akt^{PR57} was decreased to a median lifespan of 56 days. None of the survival trends of these derivative

A:

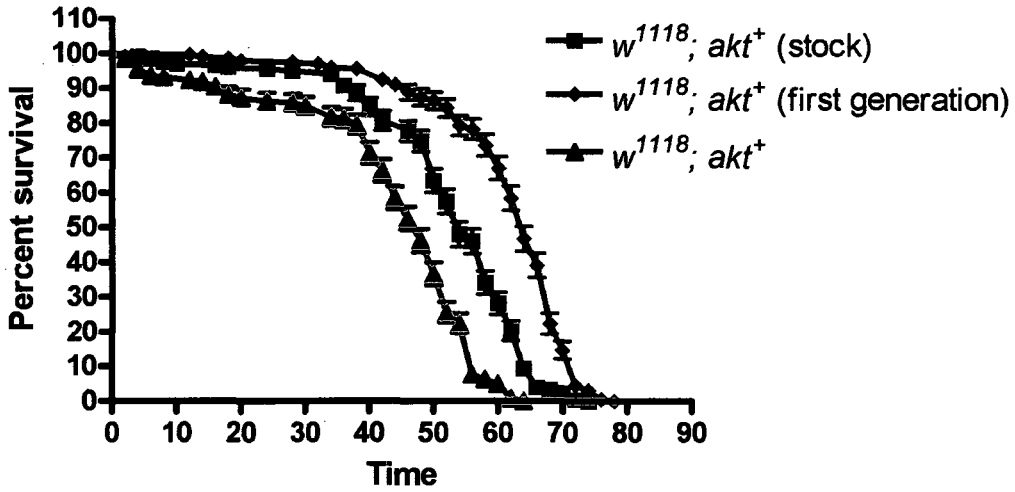

B:

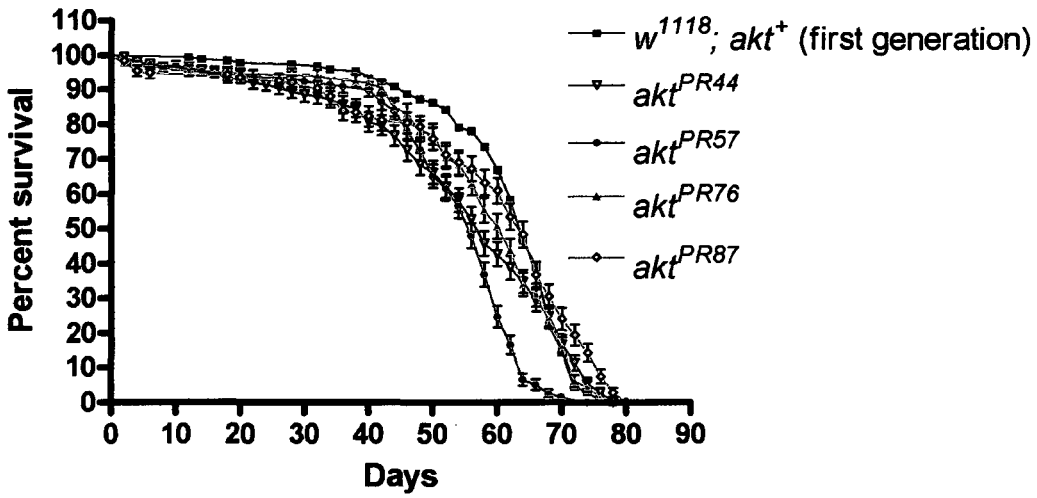

Figure 4 : **Heterozygous akt^{04226} derivatives have a lifespan similar to the control flies.** A: Longevity curves of control lines. The first generation of w^{1118}; akt^{+} with the longest lifespan was chosen for the analysis of derivatives. B: Longevity of selective akt^{04226} derivative heterozygotes and selected control line. There was no significant difference between the lifespan of the derivatives in comparison to the control, with the exception of akt^{PR57}, which had a small reduction in lifespan.

lines were determined to be greater than the control (Table 4) created from the cross of *OrR* to w^{1118} females.

Derivatives of akt^{04226} *affect cell growth and survival in the developing Drosophila eye*

Preliminary biometric analysis of homozygous akt^{04226} derivatives was carried out prior to the creation of somatic clones of the eye. Analysis of SEM micrographs confirmed that the eyes of akt^{04226} derivative homozygotes were reduced in size. While cell number varied among derivatives, homozygotes had smaller ommatidia than controls. Decreased ommatidia size, therefore, primarily contributes to the reduction in eye size in homozygous akt^{04226} derivative adults.

In order to further analyze the effect of altered *akt* activity upon ommatidia number and size, somatic clones of the eye were created. Creation of somatic clones of the eye allows for the analysis of the homozygous phenotype in a heterozygous fly. This is extremely beneficial when the homozygous fly is normally not viable. It is also advantageous when homozygotes are developmentally delayed. In this case, the prolonged development of homozygotes may allow for compensatory mechanisms which suppress the homozygous phenotype. The suppression of the phenotype would not allow for a complete analysis and thus the clonal analysis method is ideal for a second investigation into the size difference between akt^{04226} derivatives and controls.

The process of creating somatic clones requires the presence of a FLP recombinase recognition target site (FRT) near the centromere of the chromosomal arm

Table 4 : Analysis of the longevity of heterozygous akt^{04226} derivatives. Survival curves were compared using the log-rank test.

Genotype	**Number of Flies Analyzed (n)**	**Median Survival (50%)**	**Maximum Lifespan (Day)**	**P-value [compared to w^+, akt^+ (first generation) control]**	**Chi-square value [compared to w^+, akt^+ (first generation) control]**	**Significantly different**
w^{1118}; akt^+ (stock)	202	54	74	N/A	N/A	N/A
w^{1118}	219	48	64	N/A	N/A	N/A
w^{1118}; akt^+ (first generation)	197	64	78	N/A	N/A	N/A
akt^{PR44}	201	58	78	0.1628	1.948	NO
akt^{PR57}	198	56	74	<0.0001	89.92	YES
akt^{PR76}	197	62	78	0.2287	1.449	NO
akt^{PR87}	174	64	80	0.0549	3.684	NO

where the gene of interest is located, and FLP recombinase (FLP) driven by a tissue-specific driver (Theodosiou and Xu 1998). The akt^{04226} derivatives, and the selected FRT sites, are located on chromosome 3R. As we want to analyze the phenotype of the homozygous tissue in the eye, we require FLP recombinase expression in the eye. Two lines were used for this purpose. The first line, having the genotype $y^{d2}\ w^{1118}$; $P\{ry^{+t7.2}=ey\text{-}FLP.N\}^{2}$, $P\{GMR\text{-}lacZ.C(38.1)\}^{TPN1}$; $P\{ry^{+t7.2}=neoFRT\}^{82B}$, $P\{w^{+t*}\ ry^{+t*}=white\text{-}un1\}^{90E}$, $l(3)cl\text{-}R3^{1}/TM6B$, $P\{y^{+t7.7}\ ry^{+t7.2}=Car20y\}^{TPN1}$, Tb^{1} (Newsome et al. 2000) is used in the first method, known as the *ey-FLP* method, and contains the eyeless promoter driving FLP recombinase expression in the eye. For this reason, it is a direct method of clone creation. The second method, the *ey-GAL4/UAS-FLP* method, uses a line with the genotype *y w;* $P\{w^{+m}=GAL4\text{-}ey.H\}^{3\text{-}8}$, $P\{w^{+mC}=UAS\text{-}FLP1.D\}^{JD1}$; $P\{ry^{+t7.2}=neoFRT\}^{82B}$, $P\{w^{+mC}=GMR\text{-}hid\}^{SS4}$, $l(3)CL\text{-}R^{1}/TM2$ (Stowers and Schwarz 1999) which indirectly regulates the transcription of FLP recombinase in the eye. In this method, the *eyeless* driver in combination with the GAL4/UAS system is used. The transcription of *GAL4* is driven in the eye via the *eyeless* promoter, the product of which binds to the UAS to enhance the transcription of the FLP recombinase. This method is more indirect than the first, as it requires an intermediate step of the GAL4/UAS system.

Analysis of SEM micrographs of somatic eye clones created by the *ey-FLP* method revealed results similar to those seen in the previous analysis of the derivative homozygote eyes (Figures 5 and 6). The akt^{04226} eye was smaller compared to the w^{1118}; *FRT* akt^{+} control, due to both smaller ommatidia numbers and size. Control somatic eye clones had an average of 711 ± 27 ommatidia, each with an average area of 223 ± 14

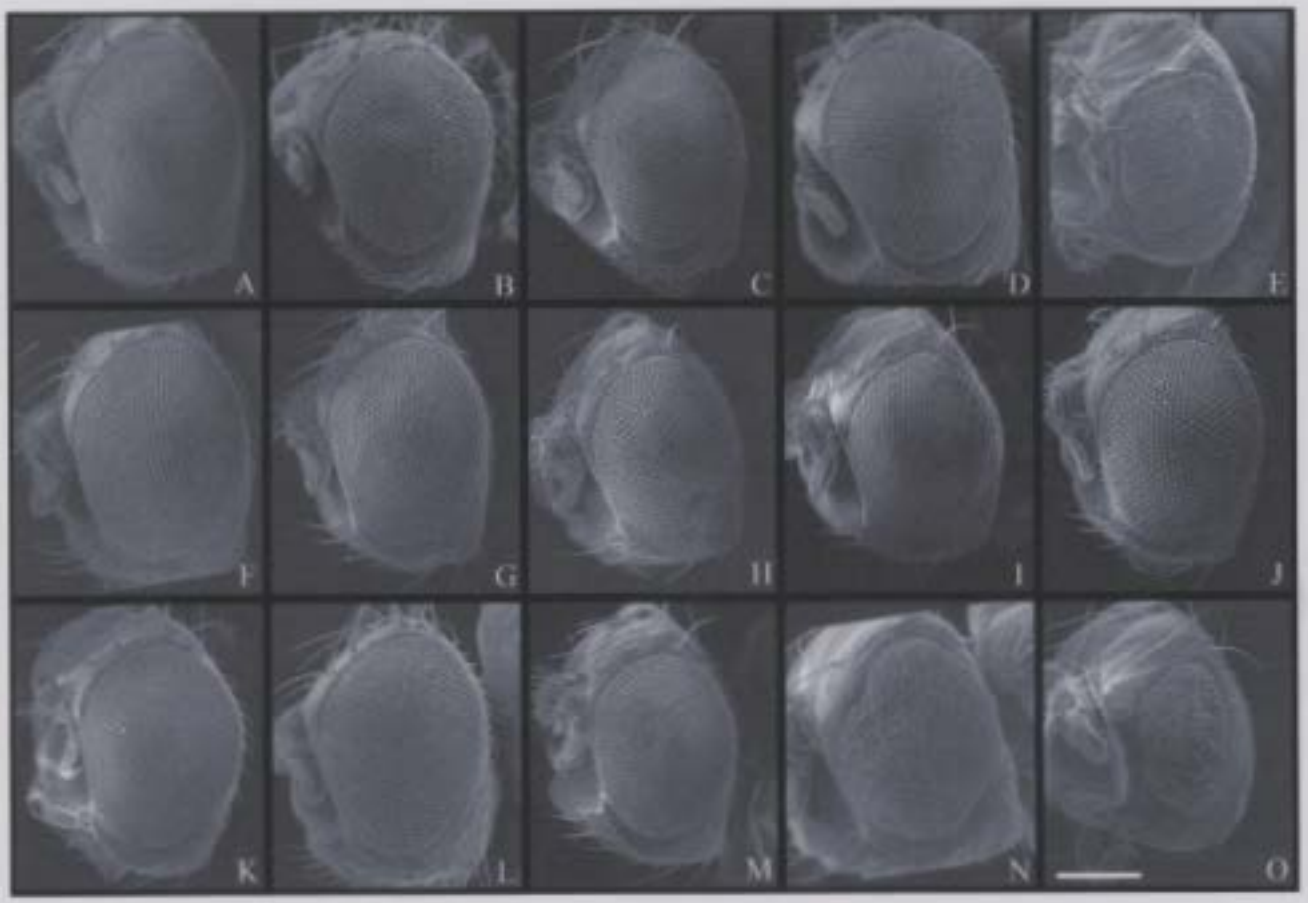

Figure 5: Eye clones of akt^{04226} derivatives range in size from small to near control and original P-element insertion line. Scanning electron images of somatic clones of the eye created by *ey-FLP* method, which involved crossing the derivatives to a line containing *ey-FLP*. Images were taken at 150X. Scale bar represents 160um. Genotypes are as follows: A: *w; FRT akt*$^{+}$ B: akt^{04226} C: akt^{PR10} D: akt^{PR12} E: akt^{PR19} F: akt^{PR24} G: akt^{PR44} H: akt^{PR52} I: akt^{PR57} J: akt^{PR60} K: akt^{PR62} L: akt^{PR76} M: akt^{PR87} N: akt^{PR174} O: akt^{PR195}

Figure 6: Analysis of akt^{04226} derivative somatic clones of the eye created via *ey-FLP* method. A: Ommatidial number varies amongst derivatives. The majority have fewer when compared to the wild-type control, but there is greater variability when compared to the original P-element insertion line. (n=3 per genotype, with the exception of akt^{PR19}, which only has one count) B: Ommatidial area of the derivatives varies but is mostly smaller than the wild-type control, with greater variation compared to the original P-element insertion line. (n=9 per genotype, with the exception of akt^{PR19}, which only has three counts) C: Bristle number of the derivatives follows a similar trend to the number of ommatidia. (n=3 per genotype, with the exception of akt^{PR19}, which only has one count). Error bars represent standard error of the mean.

A:

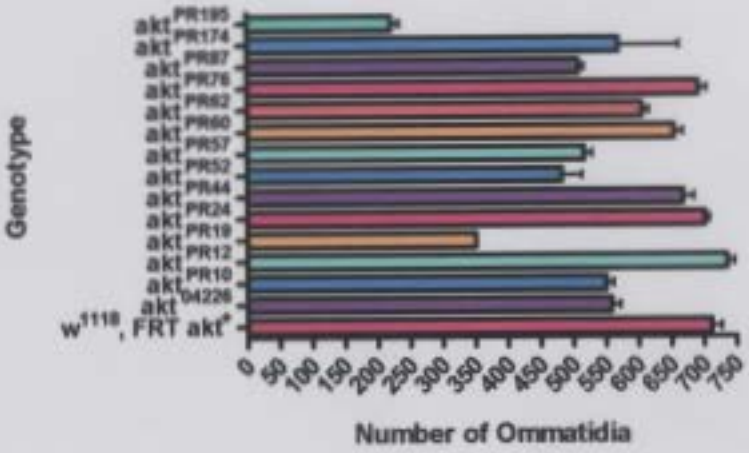
Genotype
akt PR195
akt PR174
akt PR87
akt PR76
akt PR62
akt PR60
akt PR57
akt PR52
akt PR44
akt PR24
akt PR19
akt PR12
akt PR10
akt 04226
akt
w1118, FRT akt+
0 50 100 150 200 250 300 350 400 450 500 550 600 650 700 750
Number of Ommatidia

B:

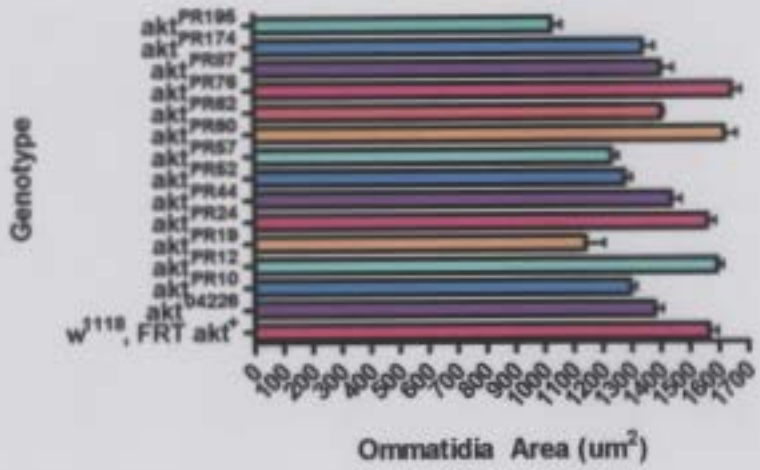
Genotype
akt PR196
akt PR174
akt PR87
akt PR76
akt PR62
akt PR60
akt PR57
akt PR52
akt PR44
akt PR24
akt PR19
akt PR12
akt PR10
akt 04226
akt
w1118, FRT akt+
0 100 200 300 400 500 600 700 800 900 1000 1100 1200 1300 1400 1500 1600 1700
Ommatidia Area (um2)

C:

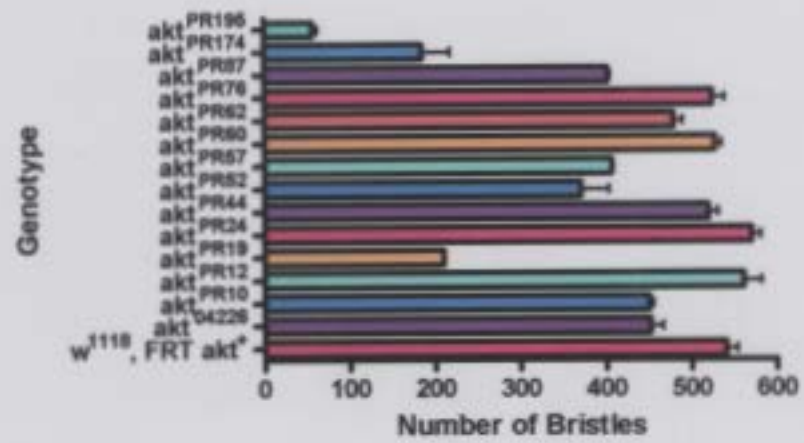
Genotype
akt PR196
akt PR174
akt PR87
akt PR76
akt PR62
akt PR60
akt PR57
akt PR52
akt PR44
akt PR24
akt PR19
akt PR12
akt PR10
akt 04226
akt
w1118, FRT akt+
0 100 200 300 400 500 600
Number of Bristles

um^2, with an average bristle number of 540 ± 24. The akt^{04226} line, in comparison, had an average of 558 ± 24 ommatidia per eye, each with an average area of 196 ± 12 um^2, and an average bristle number of 452 ± 25. In all categories the P-element insertion line was statistically smaller than the control. In addition to this, the akt^{04226} line exhibited a some abnormal ommatidia patterning, as well as misshapen ommatidial cells, which was not observed in the control somatic eye clones.

The derivative alleles were grouped based on the pattern of ommatidia number and size when compared to the w^{1118}; *FRT* akt^{+} control. Those with phenotypes which had both smaller and fewer ommatidia than the control included akt^{PR10}, akt^{PR19}, akt^{PR44}, akt^{PR52}, akt^{PR57}, akt^{PR62}, akt^{PR87}, akt^{PR174}, and akt^{PR195}. A few derivatives had eyes that were larger than control eyes. These include akt^{PR12}, akt^{PR24}, akt^{PR60} and akt^{PR76}. akt^{PR12} was larger due to a greater number of larger ommatidia. akt^{PR24} was larger due to the number of ommatidia, but not in the size of ommatidia. Both akt^{PR60} and akt^{PR76} were larger due to an increase in the size of their ommatidia, but not in number. Bristle numbers showed the same trends as ommatidia numbers, not surprisingly, as these develop concurrently. Observations of misshapen ommatidia and/or irregular ommatidial patterns indicated that most akt^{04226} derivatives displayed a small number of irregular ommatidia, while three genotypes, akt^{PR19}, akt^{PR174} and akt^{PR195} , displayed a greater degree of irregularity.

The somatic eye clone derivative alleles from the *ey-FLP* clonal method in comparison to the original P-element insertion line akt^{04226}, were grouped by the number and size of their ommaitdia. The derivatives that had a decrease in both ommatidial number and size compared to akt^{04226} include akt^{PR10}, akt^{PR19}, akt^{PR52}, akt^{PR57} and akt^{PR195}.

Some genotypes had an increase in both cell number and size and these included akt^{PR12}, akt^{PR24}, akt^{PR44}, akt^{PR60}, akt^{PR62} and akt^{PR76}. The derivative akt^{PR174} had a greater number of ommatidia, but they were smaller in size. The opposite effect, larger ommatidia but fewer in number, was exhibited by akt^{PR87}. While the grouping of derivatives compared to the w^{1118}; *FRT* akt^{+} control was more variable when compared to the original P-element insertion line, the majority of the derivatives were grouped as either having an increase in cell number and size, or a decrease in both. Only two genotypes differed in only one of these categories. This indicates that phenotypes observed in the derivatives may be subtle in comparison to the P-element insertion line, but are nonetheless meaningful.

The results from the *ey-GAL4/UAS-FLP* generated eye clones were comparable to those from the *ey-FLP* method (Figures 7 and 8). The w^{1118}; *FRT* akt^{+} control eye had an average number of ommatidia of 704 ± 6, with an average area each of 212 ± 7 um^2 and average number of bristles of 563 ± 14. This, compared to the same control in the *ey-FLP* method of clonal analysis, shows a decreased number and size of ommatidia. The number of bristles is greater in somatic clones of eye created via this method. The original P-element insertion line eye clone, made via the *ey-GAL4/UAS-FLP* method, had an average of 508 ± 35 ommatidia which averaged 179 ± 8 um^2 in size, and an average bristle number of 377 ± 19. All of these values are significantly smaller than the control values created by this eye clone method, as well as those from the P-element insertion line from the *ey-FLP* method.

The derivatives from this method can be grouped based on the number and size of the ommatidia in comparison to the control. Differences in the number of bristles were

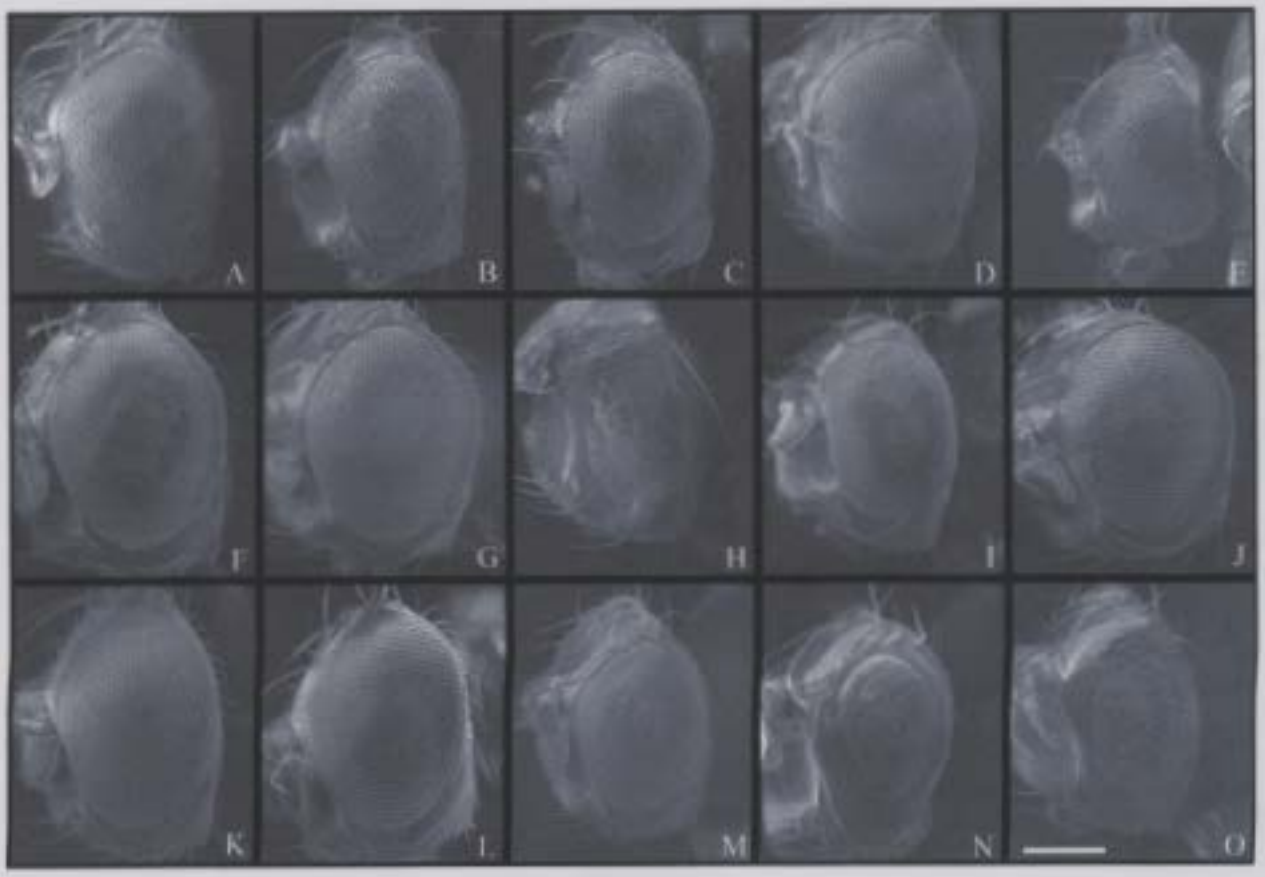

Figure 7: Eye clones of *akt*^{04226} derivatives range in size from small to near the control and the original P-element insertion line. Scanning electron images of somatic clones of the eye created by the *ey-GAL4/UAS-FLP*, which involved crossing the derivatives to a line containing *ey-GAL4* and *UAS-FLP*. Images were taken at 150X. Scale bar represents 160um. Genotypes are as follows: A: w^{1118}; *FRT akt*$^{+}$ B: *akt*^{04226} C: *akt*^{PR10} D: *akt*^{PR12} E: *akt*^{PR19} F: *akt*^{PR24} G: *akt*^{PR44} H: *akt*^{PR52} I: *akt*^{PR57} J: *akt*^{PR60} K: *akt*^{PR62} L: *akt*^{PR76} M: *akt*^{PR87} N: *akt*^{PR174} O: *akt*^{PR195}

Figure 8: Analysis of *akt*^{04226} derivative somatic clones of the eye created via the *ey-GAL4/UAS-FLP* method. A: Ommatidia number varies amongst derivatives. The majority have fewer when compared to the control, but there is greater variability when compared to the original P-element insertion line (n=3 for each genotype). B: Ommatidia area of the derivatives varies but is mostly smaller than the control, with greater variation compared to the original P-element insertion line (n=9 for each genotype). C: Bristle number of the derivatives shows a similar trend to the number of ommatidia (n=3 for each genotype). Error bars represent standard error of the mean.

A:

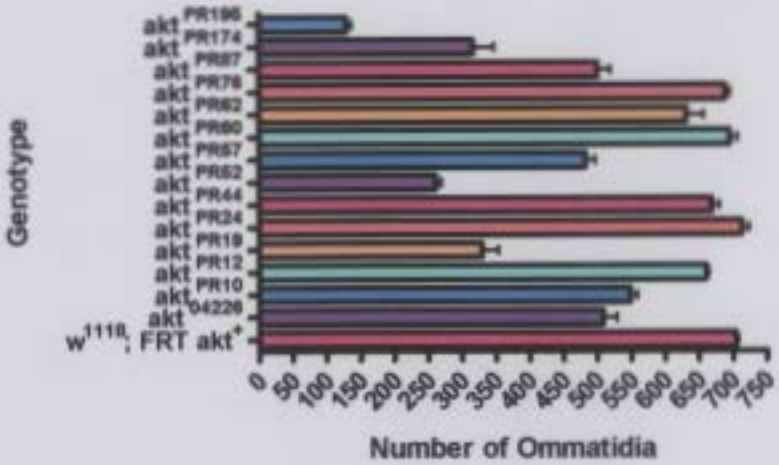
Genotype
akt PR196
akt PR174
akt PR87
akt PR76
akt PR62
akt PR60
akt PR57
akt PR52
akt PR44
akt PR24
akt PR19
akt PR12
akt PR10
akt 04226
akt
w1118; FRT akt+
0 50 100 150 200 250 300 350 400 450 500 550 600 650 700 750
Number of Ommatidia

B:

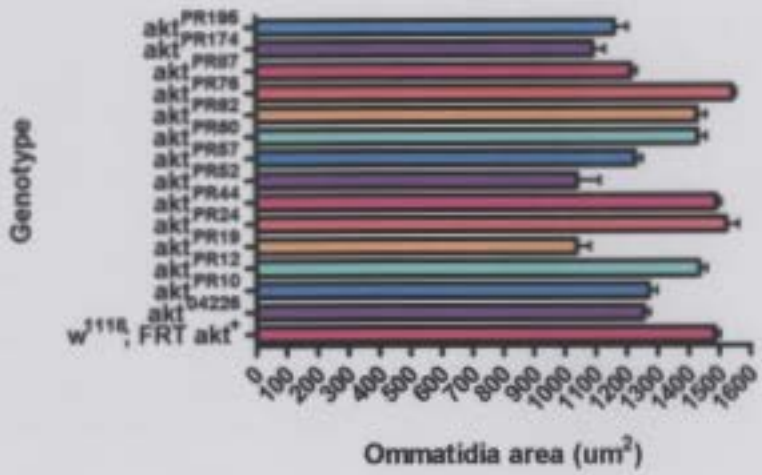
Genotype
akt PR196
akt PR174
akt PR87
akt PR76
akt PR62
akt PR60
akt PR57
akt PR52
akt PR44
akt PR24
akt PR19
akt PR12
akt PR10
akt 04226
akt
w1118; FRT akt+
0 100 200 300 400 500 600 700 800 900 1000 1100 1200 1300 1400 1500 1600
Ommatidia area (um2)

C:

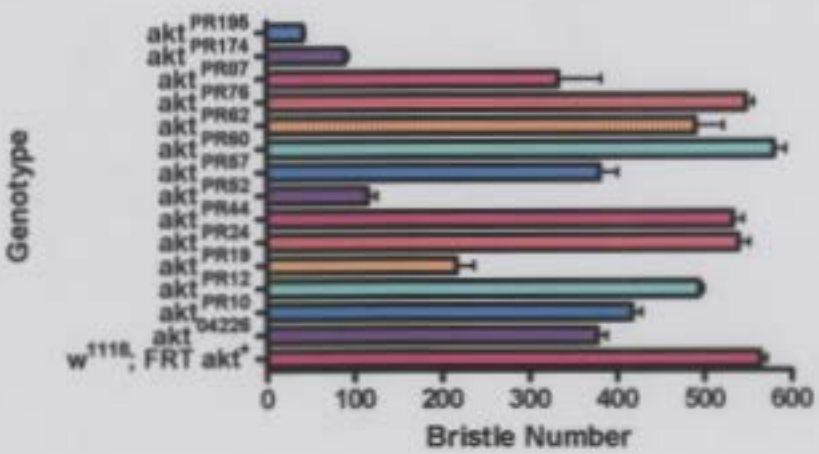
Genotype
akt PR196
akt PR174
akt PR87
akt PR76
akt PR62
akt PR60
akt PR57
akt PR52
akt PR44
akt PR24
akt PR19
akt PR12
akt PR10
akt 04226
akt
w1118; FRT akt+
0 100 200 300 400 500 600
Bristle Number

not used in the grouping as these data generally resembled the ommatidia number results. The majority of the derivatives had both fewer and smaller sized ommatidia when compared to the control. This group included akt^{PR10}, akt^{PR12}, akt^{PR19}, akt^{PR52}, akt^{PR57}, akt^{PR60}, akt^{PR62}, akt^{PR87}, akt^{PR174} and akt^{PR195}. This group now includes akt^{PR12} and akt^{PR60}, as it did not in the similar category in the *ey-FLP* method, and has lost the derivative akt^{PR44}, which was a member of this category in the *ey-FLP* eye clone analysis. akt^{PR12} and akt^{PR60} appear phenotypically similar to the control, so it is interesting that they fell into this category with this method, as before they had a greater number and size of ommatidia than the control.

The rest of the derivatives, when assessed by this method were, had values either larger than the control in both number and size, or only in size. The derivative akt^{PR24} was greater in both categories, as it did when assessed by the *ey-FLP* method. The last two derivatives, akt^{PR44} and akt^{PR76}, had larger ommatidia, but fewer of them. As mentioned earlier, akt^{PR44} had smaller values for both categories using the *ey-FLP* analysis, and akt^{PR76} had larger values in both categories. Each of the derivatives and controls showed some abnormal ommatidial patterning and shape when assessed by this method. Ommatidia disarray was more frequent than observed when using the *ey-FLP* eye clone method. The derivatives which had the most irregular ommatidia area and shape was akt^{PR19}, akt^{PR52}, akt^{PR174} and akt^{PR195}. This group includes the same three derivatives that displayed the irregular patterning and shape when assessed by the *ey-FLP* method, with the addition of one more derivative, akt^{PR52}.

Comparison of the derivatives to the original P-element insertion line resulted in grouping the derivatives into two categories: those with smaller eyes having fewer

ommatidia that were smaller in size, and those with larger eyes due to larger ommatidia present in greater numbers. The derivatives which were smaller than the P-element insertion line were akt^{PR19}, akt^{PR52}, akt^{PR57}, akt^{PR87}, akt^{PR174} and akt^{PR195}. All of these derivatives also had smaller values in comparison to the wild-type control. The rest of the derivatives had larger eyes than the original P-element insertion line based on both ommatidia number and size. These included the derivatives akt^{PR10}, akt^{PR12}, akt^{PR24}, akt^{PR44}, akt^{PR60}, akt^{PR62} and akt^{PR76}. Compared to the control, the derivatives akt^{PR10}, akt^{PR12}, akt^{PR60} and akt^{PR62} had smaller eyes in both number and size of ommatidia, meaning they fall between the control and the P-element insertion line. The derivatives akt^{PR44} and akt^{PR76} had fewer but larger ommatidia compared to the control, and therefore are in between the values for the control and P-element insertion line when it comes to ommatidia number rather than size. The derivative akt^{PR24} was greater in both categories compared to both the control and akt^{04226}.

Both methods for creating somatic clones of the eye were effective in revealing the true nature of the derivative phenotype compared to analysis of the homozygous derivative adults. The main difference between clonal methods was the expression of FLP recombinase, the enzyme required for recombination and creation of homozygous eye tissue. In the *ey-FLP* method, this enzyme was expressed directly via the eyeless promoter. While this method gave a better assessment of the homozygous derivative phenotype compared to the homozygotes alone, the second method was more sensitive. The *ey-GAL4/UAS-FLP* method had the *eyeless* promoter expressed in an indirect manner through the UAS-GAL4 system. The addition of this system allows the

production of more FLP recombinase, and therefore is more sensitive to any growth alterations observed with the akt^{04226} derivatives.

Comparison of the control and several of the derivatives that gave an obvious phenotype illustrated the difference in the sensitivity of the two methods. The control in the analysis of homozygote adults had an ommatidia count of 648 ± 4 and size of 239 ± 11 um^2. In comparison to the clonal analysis, there are fewer but larger ommatidia. The derivative akt^{PR52} gave an obvious phenotype as a somatic eye clone, but a more subtle phenotype as a homozygous adult. The homozygous analysis gave an ommatidia count of 554 ± 6 with an average size of 197 ± 7 um^2. The first clonal analysis of this genotype gave a count of 482 ± 55 and size of 182 ± 10 um^2, which is significantly less. The second method gave this genotype a count of 261 ± 15 and size of 148 ± 32 um^2, again significantly smaller values. These differences confirmed the sensitivity of the clonal analysis in comparison to analysis of the homozygotes, but also show the difference in sensitivity between clonal methods.

Other derivatives which had obvious phenotypes as somatic eye clones included akt^{PR19} and akt^{PR195}. These derivatives, as well as the original P-element insertion line akt^{04226}, were not analyzed as homozygotes because they were not viable enough to collect a sufficient number of males for imaging. The clonal analysis was beneficial in this case, as it allowed these phenotypes to be observed and measured. The data obtained for the clonal analyses, and the trends observed from this data, is summarized in tables 5 and 6.

Table 5: Summary of ommatidia number and size, and bristle numbers, obtained for each derivative in the two clonal analyses of eye tissue. Omm = ommatidia.

Genotype	Clonal Analysis: *ey-FLP* Method			Clonal Analysis: *ey-GAL4/UAS-FLP* Method		
	Omm#	**Omm Area**	**Bristle #**	**Omm#**	**Omm Area**	**Bristle #**
w; akt^{+}	711 ± 27	223 ± 14	540 ± 24	704 ± 6	212 ± 7	563 ± 14
akt^{04226}	558 ± 24	196 ± 12	452 ± 25	508 ± 35	179 ± 8	377 ± 19
akt^{PR10}	550 ± 20	185 ± 9	450 ± 8	548 ± 18	181 ± 12	417 ± 20
akt^{PR12}	735 ± 19	227 ± 9	561 ± 36	660 ± 7	204 ± 11	494 ± 9
akt^{PR19}	351	162 ± 16	210	329 ± 43	148 ± 19	216 ± 36
akt^{PR24}	702 ± 12	222 ± 12	570 ± 19	713 ± 19	217 ± 16	539 ± 22
akt^{PR44}	668 ± 29	205 ± 14	520 ± 19	668 ± 20	212 ± 7	533 ± 21
akt^{PR52}	482 ± 55	182 ± 10	371 ± 57	261 ± 15	148 ± 32	115 ± 18
akt^{PR57}	517 ± 22	175 ± 10	407 ± 1	483 ± 25	175 ± 10	380 ± 36
akt^{PR60}	654 ± 24	231 ± 18	527 ± 13	695 ± 20	204 ± 13	580 ± 24
akt^{PR62}	605 ± 19	200 ± 5	479 ± 19	632 ± 43	204 ± 12	490 ± 55
akt^{PR76}	692 ± 22	235 ± 14	524 ± 25	689 ± 13	220 ± 4	548 ± 15
akt^{PR87}	508 ± 15	200 ± 19	402 ± 5	501 ± 33	173 ± 8	333 ± 85
akt^{PR174}	570 ± 162	191 ± 17	184 ± 58	316 ± 55	156 ± 18	89 ± 9
akt^{PR195}	221 ± 22	146 ± 15	56 ± 10	129 ± 14	166 ± 19	42 ± 4

Table 6: Comparison of the three methods of analysis of akt^{04226} derivative eye tissue.

Comparison of derivatives to the control				
	Both smaller number and size of ommatidia	**Both greater number and size of ommatidia**	**Number of ommatidia is smaller; size of ommatidia is greater**	**Size of ommatidia is smaller, number of ommatidia is greater**
***akt*^{04226} derivatives as homozygous adults**	*akt*^{PR10}, *akt*^{PR24}, *akt*^{PR52}, *akt*^{PR57}, *akt*^{PR60}, *akt*^{PR62}, *akt*^{PR87}	none	*akt*^{PR12}	*akt*^{04226}, *akt*^{PR44}, *akt*^{PR76}
Clonal analysis, *ey-FLP* method	*akt*^{04226}, *akt*^{PR10}, *akt*^{PR19}, *akt*^{PR24}, *akt*^{PR44}, *akt*^{PR52}, *akt*^{PR57}, *akt*^{PR60}, *akt*^{PR62}, *akt*^{PR87}, *akt*^{PR174}, *akt*^{PR195}	*akt*^{PR12}	*akt*^{PR76}	None
Clonal analysis, *ey-GAL4/UAS-FLP* method	*akt*^{04226}, *akt*^{PR10}, *akt*^{PR12}, *akt*^{PR19}, *akt*^{PR52}, *akt*^{PR57}, *akt*^{PR60}, *akt*^{PR62}, *akt*^{PR76}, *akt*^{PR87}, *akt*^{PR174}, *akt*^{PR195}	*akt*^{PR24}	*akt*^{PR44} (area same)	None
Comparison of the derivatives to the original P-element insertion line, *akt*^{04226}				
	Both smaller number and size of ommatidia	**Both greater number and size of ommatidia**	**Number of ommatidia is smaller; size of ommatidia is greater**	**Size of ommatidia is smaller, number of ommatidia is greater**
***akt*^{04226} derivatives as homozygous adults**	*akt*^{PR10}, *akt*^{PR24}, *akt*^{PR52}, *akt*^{PR57}, *akt*^{PR60}, *akt*^{PR62}, *akt*^{PR87}	none	*akt*^{PR12}, *akt*^{PR44}, *akt*^{PR76}	None
Clonal analysis, *ey-FLP* method	*akt*^{PR10}, *akt*^{PR19}, *akt*^{PR52}, *akt*^{PR57}, *akt*^{PR195}	*akt*^{PR12}, *akt*^{PR24}, *akt*^{PR44}, *akt*^{PR60}, *akt*^{PR62}, *akt*^{PR76}	*akt*^{PR87}	*akt*^{PR174}
Clonal analysis, *ey-GAL4/UAS-FLP* method	*akt*^{PR19}, *akt*^{PR52}, *akt*^{PR57}, *akt*^{PR87}, *akt*^{PR174}, *akt*^{PR195}	*akt*^{PR10}, *akt*^{PR12}, *akt*^{PR24}, *akt*^{PR44}, *akt*^{PR60}, *akt*^{PR62}, *akt*^{PR76}	none	none

The foxo mutant adults are sensitive to amino-acid starvation

As *foxo* mutant larvae have been shown to be sensitive to amino-acid starvation when compared to wild-type controls and heterozygous *foxo* mutants (Kramer 2005), a similar experiment was carried out with amino-acid starvation beginning at eclosion. As for the larval experiment, the control organisms were generated by crossing males from the w^{1118} line to wild-type female virgins of the *OrR* stock. The resultant offspring had the genotype of $w^{+}; foxo^{+}$. Heterozygous mutants were obtained by crossing the w^{1118} wild-type line to either $foxo^{21}$ or $foxo^{25}$ flies, while transhomozygous *foxo* mutants were obtained by crossing the $foxo^{21}$ and $foxo^{25}$ lines together. The control had a median survival value of 22 days and 0% survival by 46 days. Upon comparison to these control flies, heterozygous *foxo* mutants show no significant difference in lifespan when aged on starvation media. The median lifespan for heterozygous flies was between days 20 and 21 with 0% survival by day 50 (Figure 9). Statistical analysis of heterozygous lines compared to each other and the control reveal no significant difference between either, thus heterozygous *foxo* mutants survive as well as wild-type flies on amino-acid starvation medium (Table 7).

In comparison to the heterozygotes, transhomozygotes show a significantly reduced lifespan compared to control flies (Figure 9). The median lifespan for transhomozygotes is at day 16 and their 0% survival point is at day 38. This experiment was carried out using the reciprocal crosses, which gave similar results.

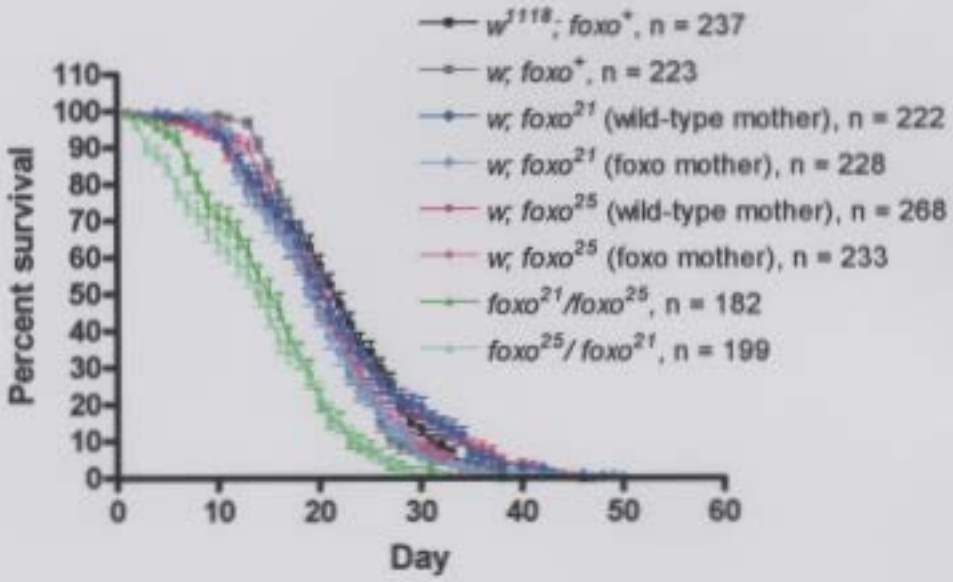

Figure 9 : The transhomozygous *foxo* mutants do not live as long as heterozygous mutants or controls under conditions of nutritional stress. Statsitical analysis reveals there is no significant difference between heterozygous mutants and controls. Transhomozygotes live for a significantly shorter period of time. Reciprocal crosses are shown. Error bars represent standard error of the mean.

Table 7: Analysis of the longevity of *foxo* mutants under conditions of amino-acid starvation. Survival curves were compared using log-rank test.

Genotype	**Number of Flies Aged (n)**	**Median Lifespan (50%)**	**Maximum Lifespan (100%)**	**P-value: compared to the control (w^+, $foxo^+$)**	**Chi-square value: compared to the control (w^+, $foxo^+$)**	**Significantly different**
$w^+; foxo^+$	237	22	46	N/A	N/A	N/A
$foxo^+/foxo^{21}$	222	21	66	0.3614	0.8331	No
$foxo^{21}/foxo^+$	222	21	50	0.4249	0.6366	No
$foxo^+/foxo^{25}$	268	20	42	0.9440	0.004936	No
$foxo^{25}/foxo^+$	268	20	48	0.8087	0.05863	No
$foxo^{21}/foxo^{25}$	182	16	38	<0.0001	65.66	Yes
$foxo^{25}/foxo^{21}$	182	16	39	<0.0001	62.33	Yes

The foxo mutants have a greater mass in comparison to control flies

In order to determine if *foxo* plays a role in the control or maintenance of adult size upon protein starvation, *foxo* mutant adults were starved for 96 hours, then mass was determined. Control flies were obtained in the same manner as discussed for the *foxo* starvation experiment, and were of the genotype w^+; $foxo^+$. These flies, on average, weighed 620 ± 132 ug when fed, and 465 ± 109 ug when starved. Heterozygous mutants, also obtained from the same crosses as described in the starvation experiment section, weighed between 680 ± 70 and 770 ± 66 ug when fed, and between 530 ± 152 and 730 ± 92 ug when starved. These numbers include the mass of both the *w; foxo*^{21}/+ and *w; foxo*^{25}/+ mutants. Overall, both heterozygote genotypes weighed more than the controls when fed or starved (Figure 10). The transhomozygous mutants maintained a weight between 690 ± 112 and 755 ± 123 ug on average when fed, and a weight of 610 ± 102 to 640 ± 88 ug on average when starved. This weight is similar to the heterozygous controls in the fed condition, but is less than the heterozygous mutants and greater than the control flies under starvation conditions (Figure 10).

Statistical analysis of this data included paired t-tests between the fed and starved condition, the fed mutants and the fed control, the starved mutants and the starved control, heterozygotes and transhomozygotes under both conditions, and between reciprocal crosses (Table 8). Taken as a whole, the difference between the fed and starved conditions, for all genotypes, was significant, with a p-value of 0.0229. It was expected that flies which were starved would be smaller than those which were fed for 96 hours, due to lack of nutrients. Secondly, a comparison of the mutant genotypes to the

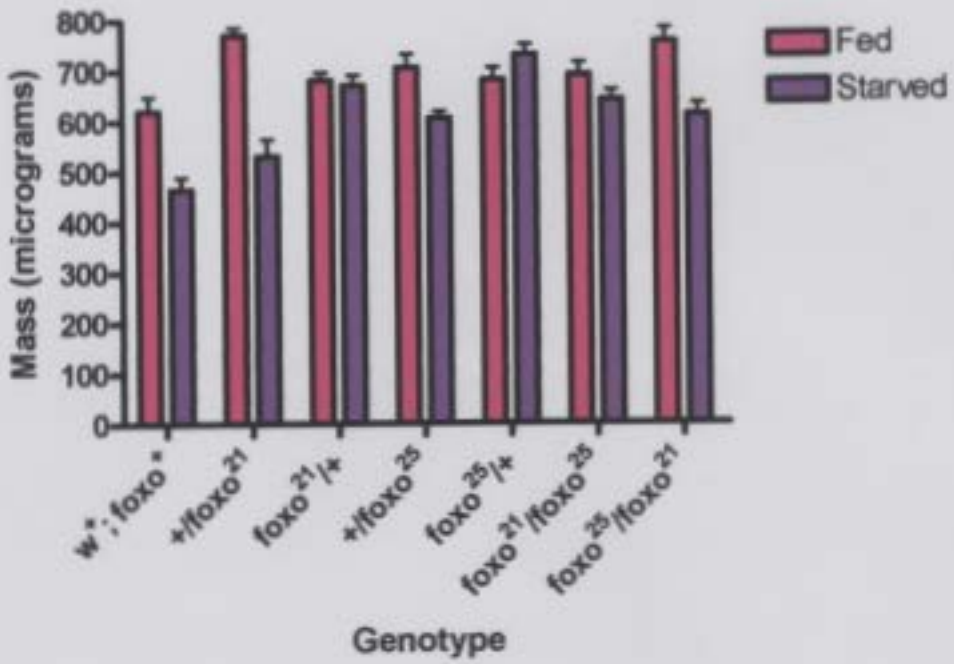

Figure 10: The *foxo* mutants are greater in mass than control flies and exhibit a possible maternal effect. Flies were weighed both after feeding for 96 hours or after undergoing 96 hours of amino-acid withdrawl. The *foxo* mutant heterozygotes and homozygotes weighed more than controls under both conditions. Some genotypes did not lose mass upon starvation. Statistical analysis also revealed a possible maternal effect. Error bars represent standard error of the mean. n = 20 for all genotypes.

Table 8: Analysis of mass of *foxo* mutants under fed and starved conditions. Statistics compiled through paired, one-tailed t-test comparisons. Results are p-values. ns = not significant and s=significant.

Genotype (Parental/Maternal)	**Fed data compared to fed control**	**Starved data compared to Starved control**	**Fed heterozygotes compared to fed transhomozygotes (*foxo*^{21}/*foxo*^{25} and *foxo*^{25}/^{21} respectively)**	**Starved heterozygotes compared to transhomozygotes (*foxo*^{21}/*foxo*^{25} and *foxo*^{25}/*foxo*^{21} respectively)**	**Fed reciprocals compared**	**Starved reciprocals compared**
foxo^{21}/*foxo*$^{+}$	0.0276, ns	<0.0001, s	0.3667, ns and 0.0140, y	0.1246, ns and 0.0586, ns	<0.0001, s	<0.0001, s
foxo^{+}/*foxo*^{21}	<0.0001, s	0.0921, ns	0.0047, y and 0.318, ns	0.0012, s and 0.0518, ns		
foxo^{25}/*foxo*$^{+}$	0.0843, ns	<0.0001, s	0.3331, ns and 0.0525, ns	0.0029, s and 0.0003, s	0.2775, ns	<0.0001, s
foxo^{+}/*foxo*^{25}	0.0100, s	0.0002, s	0.3257, ns and 0.1208, ns	0.0346, s and 0.4241, ns		
foxo^{21}/*foxo*^{25}	0.0094, s	<0.0001, s	N/A	N/A	0.0871, ns	0.1649, ns
foxo^{25}/*foxo*^{21}	0.0016, s	<0.0001, s	N/A	N/A		
All fed data compared to all starvation data				0.0229, s		

control in the fed condition revealed that both of the transhomozygotes were significantly different compared to the control. Heterozygotes were only significantly different from the control when the mother was a *foxo* mutant, which may suggest the existence of a maternal effect. The same comparisons were carried out for the starved condition. All genotypes, with the exception of the $foxo^{21}$ heterozygote (*foxo* mother), were significantly different from the control. The third statistical analysis was between the heterozygotes and transhomozygotes in both conditions. In the fed condition, both transhomozyogtes differed significantly from the $foxo^{25}$ heterozygotes, while results from the $foxo^{21}$ hetereozygotes varied. In the starved condition, the transhomozygote having the $foxo^{25}$ mother ($foxo^{21}/foxo^{25}$) was significantly different from all heterozygotes, with the exception of the $foxo^{21}$ heterozygote having a wild-type mother. The transhomozygote having $foxo^{21}$ as a mother ($foxo^{25}/foxo^{21}$) was not significantly different from any of the heterozygous genotypes, with the exception of the $foxo^{25}$ heterozygote with a wild-type mother. Comparison of the reciprocal crosses, to further analyze the possibility of a maternal effect, reveals that in the fed condition, only the $foxo^{21}$ reciprocal crosses give results significantly different from each other. In the starved condition, both $foxo^{21}$ and $foxo^{25}$ heterozygotes give results significantly different from the results of the reciprocal cross. In neither condition, there is a significant difference between transhomozygous reciprocal crosses. These results are summarized in table 8.

The level of foxo activity is upregulated in larvae during times of nutritional stress

The transgene *8XFK1tkLuc* contains a direct repeat of eight foxo binding sites upstream of the herpes simplex virus thymidine kinase minimal promoter and the gene

encoding firefly luciferase (Biggs et al. 1999). The foxo protein can bind to the eight *foxo*-responsive repeat elements leading to the transcription of the luciferase gene, which encodes a protein that, in the presence of its substrate, generates bioluminescence. This bioluminescence can be measured to indirectly monitor the presence of *foxo* activity.

The control larvae used in this experiment were derived from crosses of homozygous *FRE-luc*$^{4.2}$ flies with w^{1118}; *foxo*$^{+}$ flies. Heterozygous mutants were obtained from crossing homozygous *FRE-luc*$^{4.2}$ lines also containing one copy of either *foxo* mutant allele, *foxo*^{21} or *foxo*^{25}, to w^{1118}; *foxo*$^{+}$ flies. The transhomozygotes were obtained from crossing homozygous *FRE-luc*$^{4.2}$ lines also containing one copy of either *foxo* mutant allele, *foxo*^{21} or *foxo*^{25}, to the appropriate *foxo* mutant heterozygote. The larvae were starved from 48 hours after hatching until 96 hours after hatching. Luciferase activity was measured at 0 and 48 hours of starvation and compared.

The highest relative amount of light per milligram of protein (RLU/mg of protein) was the amount of luciferase activity observed for control larvae after 48 hours of starvation, and averaged at nearly 5,000,000 RLU/mg of protein. This value was used as an internal standard to correct for variation observed in the assays. The average RLU/mg of protein for the controls at 0 hours, and all other genotypes at both 0 and 48 hours were calculated as a percentage of this value. Error bars indicate that at 0 hours of starvation for each genotype there is little *foxo* activity. After 48 hours of starvation, *foxo* activity is upregulated in each genotype (Figure 11). As mentioned, there is a large rise in luciferase activity in the control larvae, which contain two functional copies of the *foxo*$^{+}$ gene. The heterozygous mutants, having one functional copy of *foxo*$^{+}$, experience a rise in luciferase activity, but not as great as observed in the controls. Inspection of the error

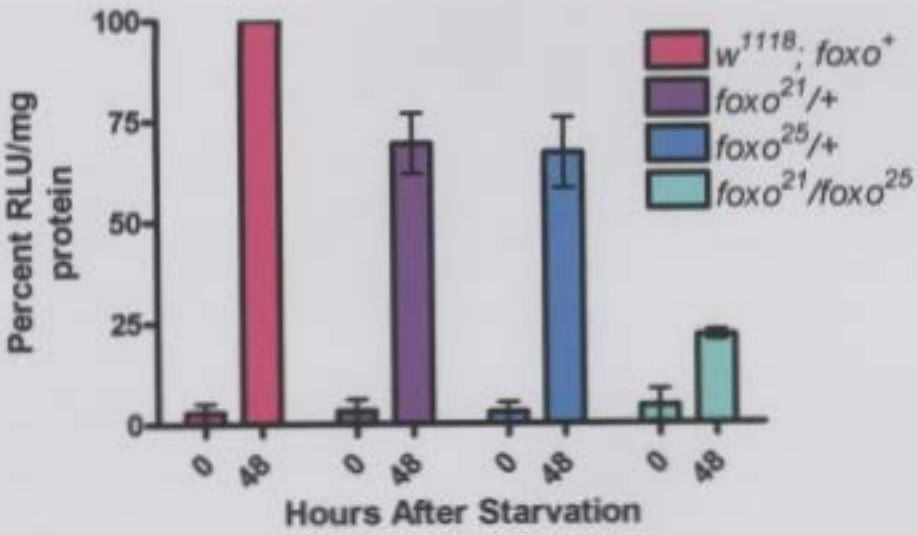

Figure 11: The level of *foxo* activity is upregulated in larvae during amino-acid starvation. Larvae were collected 48 hours after eclosion and starved of amino acids for 48 hours. Relative light per milligram of protein (RLU/mg of protein) was measured at timepoints of 0 hours after starvation and 48 hours after starvation. A significant increase in the transcription of luciferase was observed after 48 hours of starvation, indicating an upregulation of *foxo* activity. Error bars represent standard error of the mean. n = 5 for each genotype.

bars representing standard error of the mean reveals the difference between the heterozygotes data for 48 hours and the control at 48 hours is significant. The heterozygotes had an average of 69.19% (*w; foxo*^{21}) and 66.82% (*w; foxo*^{25}) of the amount of RLU/mg of protein of the control at 48 hours. The transhomozygotes still exhibited some luciferase activity after 48 hours of starvation, which averaged 21.74% of the control RLU/mg of protein activity at this timepoint. This difference is statistically significant, as indicated by t-tests (Table 9). The activity of the transhomozygotes may represent residual maternal effect. Overall *foxo* activity during conditions of nutritional stress is upregulated and varies with the number of copies of the *foxo* gene present.

The level of foxo activity in akt^{04226} *derivatives is reduced*

The protein kinase akt can exert its pro-survival nature through the phosphorylation and inhibition of one of its main downstream targets, the foxo transcription factor. Assessment of foxo activity in adult derivative lines was carried out by the luciferase assay. Lines containing the luciferase transgene in combination with the *akt*^{04226} derivative genes, were created through a series of crosses (Figure 2). Third generation adults contained the transgene on the second chromosome, and the *akt*^{04226} derivative on the third chromosome. Two versions of the luciferase transgene, versions 4.2 and 5.5, were used in the crosses, with successful lines created for each of the 13 *akt*^{04226} derivatives, as well as for the original P-element insertion line and a wild-type control. Collection of adults which contained the *FRE-luc* transgene in combination with a selection of homozygous *akt*^{04226} derivative genes was performed with the luciferase 5.5

Table 9: Analysis of the FRE-luciferase activity of *foxo* mutants under conditions of nutritional stress. Values were compared using paired t-tests. s = significantly different, ns = not significantly different.

Genotype	**Comparison of 0 Hour data to 48 Hour data**	**Comparison of 0 Hour data to Control 0 Hour data**	**Comparison of 48 Hour data to Control 48 Hour data**
w; foxo^{+}	0.0003, s	N/A	N/A
foxo^{21}*/foxo*$^{+}$	0.0102, s	0.2329, ns	0.0274, s
foxo^{25}*/foxo*$^{+}$	0.0130, s	0.4382, ns	0.0315, s
foxo^{21}*/foxo*^{25}	0.0132, s	0.2100, ns	0.0001, s

version of the lines. These included the control akt^{+}, and the derivatives akt^{PR10}, akt^{PR12}, akt^{PR44}, akt^{PR52}, akt^{PR57}, akt^{PR60} and akt^{PR76}.

The control adults, homozygous for *FRE-luc*$^{5.5}$ and of the genotype w^{+}; *FRT* akt^{+}, revealed a moderate amount of luciferase activity. These flies have two functional copies of *akt* and two functional copies of *foxo*, so this level of *foxo* activity was considered as the standard for this experiment. Compared to the control, all homozygous derivatives exhibited a lower amount of luciferase activity per amount of total protein (RLU/mg protein), thus revealing a lowered activity of *foxo* (Figure 12A). The derivatives were not significantly different from each other, but could be arbitrarily ranked based on the mean of their RLU/mg protein values. The derivative with the highest mean of RLU/mg protein was akt^{PR12}, which had a mean of 2.4 x10^{6} RLU/mg protein. This derivative also is the most phenotypically similar to the wild-type lines in clonal analysis. The derivative with the second highest mean was akt^{PR60}, with a mean of 1.9 x 10^{6} RLU/mg protein. Interestingly, this derivative also closely resembles the wild-type in clonal analysis. The third highest mean was 1.7 x 10^{6} RLU/mg protein for the akt^{PR10} allele. Following this was akt^{PR57} with a mean of 1.4 x 10^{6} RLU/mg protein. The means begin to lower with the derivative akt^{PR52} having a mean of 1.1 x10^{6}. This allele has an obviously smaller eye phenotype when compared to the control during clonal analysis. The next mean was 8.5 x 10^{5} RLU/mg protein and belonged to akt^{PR44}. The smallest mean was 4.9 x 10^{4} for the akt^{PR76} eye phenotype.

A:

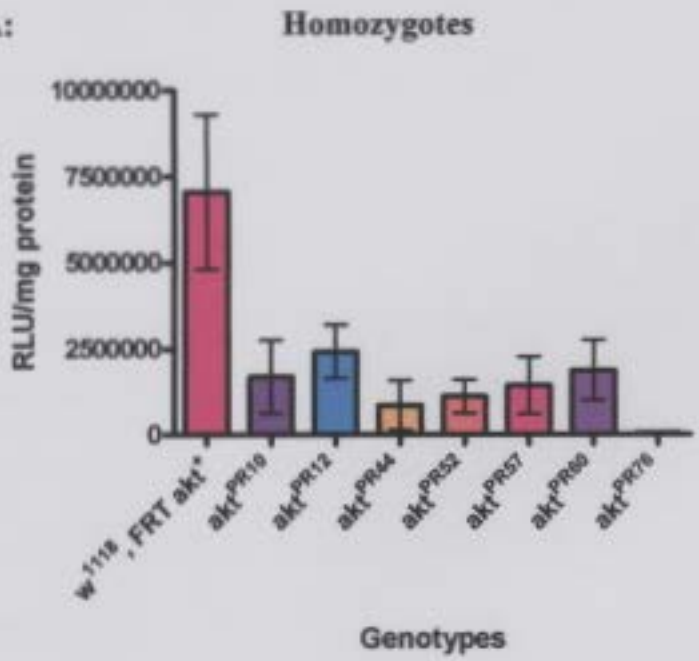

B:

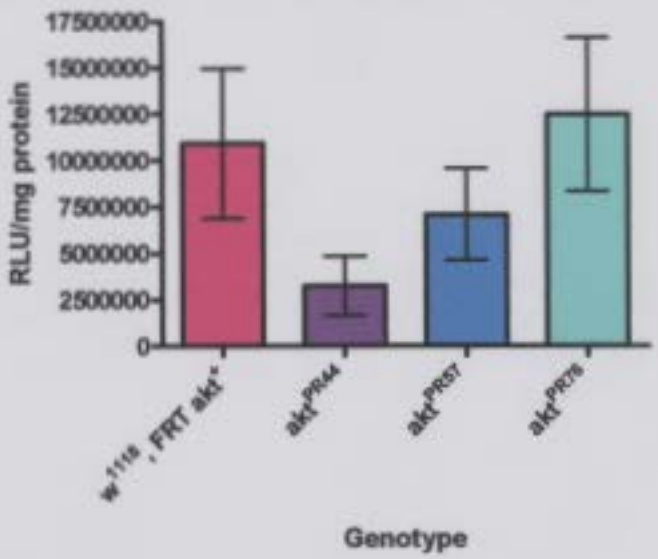

Figure 12 : Homozygous and heterozygous *akt*^{04226} derivatives have lowered luciferase activity in comparison to controls. A: Homozygous derivative adults all have a lowered relative amount of light (RLU) measured per milligram of protein, indicating a lower luciferase, and thus foxo, activity. B: Heterozygous *akt*^{04226} derivatives have a lower level of luciferase activity when compared to the control, but a greater amount compared to the homozygotes. Error bars represent standard error of the mean, n = 5 for each genotype.Statistical analysis of homozygous derivative luciferase activity compared to the control confirms the statistical significance of these results.

Statistical analysis of homozygous derivative luciferase activity compared to the control confirms the statistical significance of these results.

In addition to analysis of homozygous derivatives, heterozygous derivative adults were also examined using the *FRE-luc*$^{5.5}$ transgene (Figure 12B). The heterozygotes chosen to be analyzed were of the genotypes *akt*^{PR44}, *akt*^{PR57} and *akt*^{PR76}, along with the control line w^+, *FRT akt*$^+$, as these lines previously exhibited an extended lifespan, and were analyzed as homozygotes. The control, as before, showed a moderate amount of luciferase activity, consistent with two functional copies of *foxo*. The heterozygous derivatives have only one functional copy of *foxo*, and in comparison to the control, they generally exhibit a lower amount of luciferase activity. The derivatives *akt*^{PR44} and *akt*^{PR57} exhibited an amount of luciferase activity lower than the control, while *akt*^{PR76} revealed a level of luciferase activity comparable to the control. These results were highly variable and require further analysis. Statistical analysis of both heterozygous and homozygous *akt*^{04226} derivative luciferase assays is summarized in table 10.

Table 10: Analysis of the FRE-luciferase activity of homozygous and heterozygous akt^{04226} derivatives. Values were compared using paired t-tests.

Genotype	P-value (Compared to Control)	Significantly different
Homozygous akt^{04226} derivatives		
akt^{PR10}	0.0233	Yes
akt^{PR12}	0.0221	Yes
akt^{PR44}	0.0127	Yes
akt^{PR52}	0.0175	Yes
akt^{PR57}	0.0243	Yes
akt^{PR60}	0.0141	Yes
akt^{PR76}	0.0172	Yes
Heterozygous akt^{04226} derivatives		
akt^{PR44}	0.0293	Yes
akt^{PR57}	0.1892	No
akt^{PR76}	0.2873	No

Discussion

The akt protein kinase is a central component in insulin signaling that acts through many downstream targets to promote cell survival, growth, proliferation, angiogenesis, metabolism and migration (Manning and Cantley 2007). Analysis of the role of *akt* in growth in the developing *Drosophila melanogaster* eye has revealed that *akt*-deficient rhabdomeres exhibit a reduction in size, indicating an essential role in normal cell growth in a cell-autonomous manner (Verdu et al. 1999). Homozygous *akt* mutant eyes, and eyes overexpressing a dominant negative version of PI3K or PTEN, a negative regulator of insulin signaling, all result in small eyes (Scanga et al. 2000). Co-expression of *akt* with these dominant negative mutants was able to signifcantly suppress the reduction in cell size. Overexpression of *akt* in the developing eye leads to enlarged eyes, due to increase in the cell size but not number (Verdu et al. 1999). Therefore, *akt* is downstream of both PI3K and PTEN and functions in the control of cell size and growth.

The transcription factor foxo, an important downstream target of akt, enhances the activity of downstream targets that slow cell cycle progression, inhibit protein translation, and increase cell death (Junger et al. 2003; Kramer et al. 2003; Puig et al. 2003; Barthel et al. 2005). An increase of *foxo* activity in the eye leads to reduction in both ommatidia number and size (Junger et al. 2003; Kramer et al. 2003; Puig et al. 2003). When upstream components *akt* or *PI3K* are co-overexpressed with *foxo*, the reduction in cell number and size is rescued, to near wild-type phenotype (Kramer et al. 2003). This demonstrates roles in cell growth and size regulation for both *foxo* and *akt*.

The Drosophila eye normally consists of between 700 and 800 ommatidia, each composed of photoreceptor cells, cone cells, pigment cells, and a bristle cell group (Baker

2001). Eye development occurs when the morphogenetic furrow, a dorsoventral indentation, sweeps anteriorly across the eye disc to result in ommatidial development across the anterior/posterior axis of the eye imaginal disc. This developmental process is highly regulated and ideal for study of cell growth and survival. The initial characterization of some akt^{04226} derivatives showed small eyes, mainly due to a decrease in cell size. As the akt^{04226} derivatives are developmentally delayed (Slade 2005), experiments were designed to further analyze cell growth in these lines, without the possibility of compensatory growth due to the delay in development.

As the eye is not required for viability within a laboratory setting, generation of somatic clones in the eye allows examination of the homozygous phenotype in a heterozygous animal. This method is effective for the analysis of many homozygous lethal alleles, as well as alleles that lead to developmentally delayed adults. Two clonal methods were used to generate somatic clones of the eye, and were compared. The *ey-FLP* method utilized a direct activation of the FLP recombinase by the *eyeless* promoter. Compared to homozygous adults of the akt^{04226} derivatives, this method reveals a greater reduction in cell size and number in the adult eye. The *ey-GAL4/UAS-FLP* method, with indirect expression of the FLP recombinase via the intermediate step of the UAS/GAL4 system, allows for a greater number of the FLP recombinase to be present, therefore potentially increasing the efficiency of recombination.

In the *ey-FLP* method, the majority of akt^{04226} derivatives exhibit decreased ommatidia and bristle numbers, and ommatidia sizes compared to the akt^{+} control. Bristle number examined with *ey-FLP* clonal analysis was reduced when compared to the analysis of adult homozygotes. Bristle cells form late in eye development, which makes

them a highly sensitive indicator of alterations in cell growth. In comparison to the original P-element insertion line, the derivatives either had a greater number of larger ommatidia, or a fewer number of smaller ommatidia. Eye clones reveal that some derivatives also had altered ommatidial patterning and shape. Altogether, these results indicate the *ey-FLP* clonal method generates a more severe phenotype than developmentally delayed homozygotes. This is probably due to the ability to observe the homozygous phenotype in a heterozygous organism, and avoid any growth compensation within the developmentally delayed homozygous derivatives.

Analysis of the akt^{04226} derivatives using the *ey-GAL4/UAS-FLP* method reveals that the majority of derivatives have reduced cell number and size when compared to the ommatidia of akt^{+} flies. In most cases, the phenotype was more severe with this method. All derivatives, as well as the control, exhibited some disruption of the ommatidial array. A few of the derivatives which exhibited disarray in the *ey-FLP* method exhibit a greater amount of misshapen and irregularly patterend ommatidia in the *ey-GAL4/UAS-FLP* method. This method was the most sensitive method used to study the homozygous phenotype of the derivatives, likely due to its potential to express a greater number of the FLP recombinase when compared to the *ey-FLP* method.

The akt kinase is believed to exert its affect on cell growth predominantly through the activation of the target of rapamycin (TOR) complex, which functions as a sensor of cellular nutrient and energy levels (Ruggero and Sonenberg 2005). This activation allows for downstream targets of TOR, including S6 Kinase 1 (S6K1) and eukaryotic initiation factor 4E binding protein (4EBP), to become activated (Ruggero and Sonenberg 2005). Activated S6K1 stimulates the initiation of protein synthesis through activation of

translational machinery. While non-phosphorylated 4EBP binds tightly to the translation initiation factor eIF4E, preventing it from binding to 5'-capped mRNAs, phosphorylation by TOR leads to 4EBP releasing eIF4E, allowing it to perform its function. In addition, the akt kinase can influence cell proliferation in mammals through $p27^{kip1}$ and $p21^{Cip/WAF1}$, or likely by dacapo in Drosophila, by direct phosphorylation to sequester them to the cytoplasm by 14-3-3 proteins (Manning and Cantley 2007). $p27^{kip1}$ leads to the attenuation of the cell-cycle inhibition, and $p21^{Cip/WAF1}$ blocks cell-cycle progression. It may be through these targets that growth is altered within the akt^{04226} derivative somatic clones.

The akt kinase can control cell number in the developing eye through influence upon cell survival and proliferation. The enhancement of cell survival arises through *akt* blocking pro-apoptotic proteins, such as the protein BAD and the transcription factor *foxo* (Brunet et al. 1999; Datta et al. 1999). BAD inhibits anti-apoptotic Bcl-2 family members, but upon phosphorylation by akt, BAD is no longer able to bind to these proteins and binds to 14-3-3 proteins in the cytoplasm. A similar mechanism is active when akt phosphorylates foxo. The affinity for 14-3-3 proteins is enhanced, and this leads to foxo being drawn out of the nucleus, where it would normally function to enhance the transcription of pro-apoptotic proteins. Instead it becomes sequestered in the cytoplasm, rendering it inactive. If there is increased *foxo* activity, it can enhance the downstream transcription of one of its targets, 4EBP (Van Der Heide et al. 2004), that regulates the translation of proteins. These mechanisms may be those which are responsible for the smaller number or size of ommaitidia observed in the akt^{04226} derivatives.

Some akt^{04226} derivatives experienced an extended lifespan compared to control organisms. This result was interesting as it differed from the effects upon longevity experienced by the other alleles, both heterozygous and homozygous. In order to further investigate this, a replicate ageing assay was performed, but did not reveal a significant increase in lifespan, thus revealing these lines were as healthy as those which contain two functional copies of *akt*.

The overexpression of *foxo* phenocopies behaviour observed in larvae undergoing starvation, including developmental arrest and alterations in feeding behavior and is reversed upon discontinuation of *foxo* expression (Kramer et al. 2003). In addition, the *foxo* mutants are observed to be sensitive to oxidative stress (Junger et al. 2003) and are developmentally delayed (Kramer 2005). Due to the presence of starvation-like phenotypes in larvae overexpressing *foxo,* and the sensitivity of *foxo* mutants to stresses, *foxo* mutant larvae were assayed to determine their ability to deal with nutritional stress. The $foxo^{21}/foxo^{25}$ mutant larvae experienced a significantly shorter lifespan compared to controls having one or two functional copies of *foxo* when aged upon amino-acid deficient medium. When adults were analyzed, the heterozygotes exhibited a lifespan similar to the control, while the transhomozygous mutants had a much shorter lifespan during starvation conditions. This suggests one functional copy of *foxo* is sufficient to survive nutritional stress, and that having no *foxo* is detrimental during these conditions.

Young larvae require the *foxo* downstream target 4EBP for maximal survival during starvation (Junger et al. 2003; Tettweiler et al. 2005). The translational repressor 4EBP is expressed in response to *foxo* expression to reduce protein synthesis, to decrease cell growth and results in smaller adults. Studies of starvation in *Drosophila* have

determined the existence of the "70-hour change". This phenomenon states that if larvae are starved prior to 70 hours after egg laying, they will die. If the starvation begins after 70 hours, the larvae may develop into adults which are smaller in size (Beadle et al. 1938). The *foxo* mutants have been shown to develop into smaller than normal adults, and *foxo* is implicated as a key mediator of survival under starvation conditions. Comparison of the $foxo^{21}/+$ from reciprocal crosses suggests a possible maternal effect of *foxo* activity in this allele. *foxo* was determined to have a strong maternal contribution to the early embryo of Drosophila, but to disappear early in the blastoderm before cellularization (Lee and Frasch 2004). The bars representing the mass of heterozygous adult flies with a wild-type mother were significantly smaller than those which were created using a $foxo^{21}$ mutant mother (Table 6), suggesting a maternal effect of the $foxo^{21}$ allele upon cell growth under conditions of both nutritional stress and normal conditions.

Overexpression studies revealed that when *foxo* is upregulated, the larvae phenocopy behaviours that are observed during starvation experiments. The Staveley laboratory developed a novel luciferase assay that I used to determine the relative amounts of *foxo* activity under these conditions. This assay depends upon a transgene, which contains eight forkhead-responsive elements (FRE) upstream of the *luciferase* gene. As *foxo* is activated in the organism, it binds to the FRE elements, leading to the production of luciferase. Upon addition of the substrate luciferin, a light-emitting chemical reaction can be measured to indirectly indicate levels of *foxo* activity.

In order to determine the pattern of *foxo* activity during the time of starvation, luciferase assays of larvae at 0 and 48 hours after starvation were performed. An overall trend of increased *foxo* activity over time was observed for all genotypes. The

foxo^{21}/*foxo*^{25} mutants had a much lower level of activity compared to the heterozygous mutants, which had reduced levels of activity compared to controls. The upregulation of *foxo* activity with starvation, as well as the sensitivity of *foxo* mutants to starvation, suggests that *foxo* is required to mediate the transcription of genes that promote survival during starvation. The *foxo*^{21}/*foxo*^{25} mutants did exhibit a small increase in *foxo* activity. The residual luciferase activity seen in the absence of *foxo* may be due to maternally inherited *foxo* or to other factors that can influence gene expression from the FRE in response to amino acid withdrawal. However, *foxo* is clearly required for the full transcriptional activation of the reporter gene.

As foxo activity is repressed by phosphorylation by akt, it was predicted that foxo activity would be upregulated in the *akt*^{04226} derivatives. In order to determine the relative amount of akt activity in the derivatives, the activity of foxo was measured using the luciferase assay. The luciferase assays indicate a reduction of foxo activity in a number of *akt*^{04226} derivatives when compared to the *akt*$^{+}$ control. This was true for both homozygous and heterozygous derivatives. Overall these results give an insight to the activity of the *akt*^{04226} derivatives examined. The derivatives differed from the wild-type control, suggesting there is an alteration in *akt* activity in the derivatives. In order to confirm the direction of altered *akt* activity in these lines, further analysis is required.

While the results for the homozygous *akt*^{04226} derivatives was unexpected, it may be explained by a downstream target of *foxo*, the insulin receptor (Puig et al. 2003; Puig and Tjian 2005). When insulin signaling is high due to an influx of nutrients, foxo is exported from the nucleus and repressed. Once nutrients become unavailable, insulin signaling is turned off, allowing foxo to become active, and enhances the transcription of

the insulin receptor to allow for an increase of this protein on the cell surface. This makes the cell more sensitive to the presence of insulin, and thus able to re-initiate insulin signaling, *akt* activity, and to repress *foxo* activity. Due to the negative feedback of *foxo*, viable alleles of *akt* may have a baseline of foxo activity below control levels.

The examination of these akt^{04226} derivatives aid in further understanding the effect of altered akt activity upon cell growth. The clonal methods confirmed a role for *akt* in the control of cell size and number. Upon comparing the techniques, the *ey-GAL4/UAS-FLP* method gave more sensitive results, and thus is the more informative method to use. The transcription factor foxo was found to be important in times of nutritional stress, as transhomozygotes were sensitive to amino-acid starvation. A possible maternal effect of *foxo* upon the size of adult flies was discovered. Further analysis of this result could include the creation of germline clones of the *foxo* gene. A novel assay for the determination of foxo activity under various conditions was developed and utilized to measure foxo activity at different timepoints during starvation in *foxo* mutants and to, indirectly, measure the amount of akt activity within the derivatives. The analysis of foxo activity in flies under nutritional stress again revealed the importance of this protein in managing these conditions, as it was upregulated with increased time of starvation. The use of the luciferase assay to indirectly measure the activity of akt^{04226} derivatives allowed for some biochemical analysis of these lines. This method represents a novel and accurate way of measuring the activity of endogenous and mutant *foxo* genes. Indirectly, it can measure the activity of upstream components of the insulin pathway that regulate *foxo*, and can be used to measure the effect of environmental factors, such as age and stress, on the activity of endogenous *foxo*.

References

Abramoff, M.D., Magelhaes, P.J., Ram, S.J. 2004. Image Processing with ImageJ. *Biophotonics International* **11**(7): 36-42.

Alessi, D.R. and Cohen, P. 1998. Mechanism of activation and function of protein kinase B. *Current opinion in genetics & development* **8**(1): 55-62.

Aoyama, H., Daitoku, H., and Fukamizu, A. 2006. Nutrient control of phosphorylation and translocation of Foxo1 in C57BL/6 and db/db mice. *Int J Mol Med* **18**(3): 433-439.

Arking, R. 2005. Multiple longevity phenotypes and the transition from health to senescence. *Ann N Y Acad Sci* **1057**: 16-27.

Baker, N.E. 2001. Cell proliferation, survival, and death in the Drosophila eye. *Seminars in cell & developmental biology* **12**(6): 499-507.

Barbieri, M., Bonafe, M., Franceschi, C., and Paolisso, G. 2003. Insulin/IGF-I-signaling pathway: an evolutionarily conserved mechanism of longevity from yeast to humans. *Am J Physiol Endocrinol Metab* **285**(5): E1064-1071.

Barthel, A., Schmoll, D., and Unterman, T.G. 2005. FoxO proteins in insulin action and metabolism. *Trends Endocrinol Metab* **16**(4): 183-189.

Bartke, A. 2001. Mutations prolong life in flies; implications for aging in mammals. *Trends Endocrinol Metab* **12**(6): 233-234.

Beadle, G.W., Anderson, R.L., and Maxwell, J. 1938. A comparison of the diffusible Substances Concerned with Eye Color Development in Drosophila, Ephestia and Habrobracon. *Proceedings of the National Academy of Sciences of the United States of America* **24**(2): 80-85.

Biggs, W.H., 3rd, Meisenhelder, J., Hunter, T., Cavenee, W.K., and Arden, K.C. 1999. Protein kinase B/Akt-mediated phosphorylation promotes nuclear exclusion of the winged helix transcription factor FKHR1. *Proceedings of the National Academy of Sciences of the United States of America* **96**(13): 7421-7426.

Britton, J.S., Lockwood, W.K., Li, L., Cohen, S.M., and Edgar, B.A. 2002. Drosophila's insulin/PI3-kinase pathway coordinates cellular metabolism with nutritional conditions. *Dev Cell* **2**(2): 239-249.

Brogiolo, W., Stocker, H., Ikeya, T., Rintelen, F., Fernandez, R., and Hafen, E. 2001. An evolutionarily conserved function of the Drosophila insulin receptor and insulin-like peptides in growth control. *Curr Biol* **11**(4): 213-221.

Brunet, A., Bonni, A., Zigmond, M.J., Lin, M.Z., Juo, P., Hu, L.S., Anderson, M.J., Arden, K.C., Blenis, J., and Greenberg, M.E. 1999. Akt promotes cell survival by phosphorylating and inhibiting a Forkhead transcription factor. *Cell* **96**(6): 857-868.

Burgering, B.M. and Kops, G.J. 2002. Cell cycle and death control: long live Forkheads. *Trends Biochem Sci* **27**(7): 352-360.

Burgering, B.M. and Medema, R.H. 2003. Decisions on life and death: FOXO Forkhead transcription factors are in command when PKB/Akt is off duty. *J Leukoc Biol* **73**(6): 689-701.

Cavaliere, V., Donati, A., Hsouna, A., Hsu, T., and Gargiulo, G. 2005. dAkt kinase controls follicle cell size during Drosophila oogenesis. *Dev Dyn* **232**(3): 845-854.

Cheng, C.L., Gao, T.Q., Wang, Z., and Li, D.D. 2005. Role of insulin/insulin-like growth factor 1 signaling pathway in longevity. *World J Gastroenterol* **11**(13): 1891-1895.

Clancy, D.J., Gems, D., Hafen, E., Leevers, S.J., and Partridge, L. 2002. Dietary restriction in long-lived dwarf flies. *Science* **296**(5566): 319.

Clancy, D.J., Gems, D., Harshman, L.G., Oldham, S., Stocker, H., Hafen, E., Leevers, S.J., and Partridge, L. 2001. Extension of life-span by loss of CHICO, a Drosophila insulin receptor substrate protein. *Science* **292**(5514): 104-106.

Coelho, C.M. and Leevers, S.J. 2000. Do growth and cell division rates determine cell size in multicellular organisms? *J Cell Sci* **113 (Pt 17)**: 2927-2934.

Cohen, P. and Frame, S. 2001. The renaissance of GSK3. *Nature reviews* **2**(10): 769-776.

Culotta, V.C., Yang, M., and O'Halloran, T.V. 2006. Activation of superoxide dismutases: putting the metal to the pedal. *Biochimica et biophysica acta* **1763**(7): 747-758.

Datta, S.R., Brunet, A., and Greenberg, M.E. 1999. Cellular survival: a play in three Akts. *Genes & development* **13**(22): 2905-2927.

Day, S.J. and Lawrence, P.A. 2000. Measuring dimensions: the regulation of size and shape. *Development (Cambridge, England)* **127**(14): 2977-2987.

Dijkers, P.F., Medema, R.H., Pals, C., Banerji, L., Thomas, N.S., Lam, E.W., Burgering, B.M., Raaijmakers, J.A., Lammers, J.W., Koenderman, L., and Coffer, P.J. 2000. Forkhead transcription factor FKHR-L1 modulates cytokine-dependent transcriptional regulation of p27(KIP1). *Molecular and cellular biology* **20**(24): 9138-9148.

Dionne, M.S., Pham, L.N., Shirasu-Hiza, M., and Schneider, D.S. 2006. Akt and FOXO dysregulation contribute to infection-induced wasting in Drosophila. *Curr Biol* **16**(20): 1977-1985.

Downward, J. 2004. PI 3-kinase, Akt and cell survival. *Seminars in cell & developmental biology* **15**(2): 177-182.

Edgar, B.A. 2006. How flies get their size: genetics meets physiology. *Nat Rev Genet* **7**(12): 907-916.

Essers, M.A., Weijzen, S., de Vries-Smits, A.M., Saarloos, I., de Ruiter, N.D., Bos, J.L., and Burgering, B.M. 2004. FOXO transcription factor activation by oxidative stress mediated by the small GTPase Ral and JNK. *The EMBO journal* **23**(24): 4802-4812.

Farese, R.V. 2001. Insulin-sensitive phospholipid signaling systems and glucose transport. Update II. *Experimental biology and medicine (Maywood, NJ* **226**(4): 283-295.

Franke, T.F., Hornik, C.P., Segev, L., Shostak, G.A., and Sugimoto, C. 2003. PI3K/Akt and apoptosis: size matters. *Oncogene* **22**(56): 8983-8998.

Furukawa-Hibi, Y., Kobayashi, Y., Chen, C., and Motoyama, N. 2005. FOXO transcription factors in cell-cycle regulation and the response to oxidative stress. *Antioxid Redox Signal* **7**(5-6): 752-760.

Gao, X., Neufeld, T.P., and Pan, D. 2000. Drosophila PTEN regulates cell growth and proliferation through PI3K-dependent and -independent pathways. *Developmental biology* **221**(2): 404-418.

Garofalo, R.S. 2002. Genetic analysis of insulin signaling in Drosophila. *Trends Endocrinol Metab* **13**(4): 156-162.

Geminard, C., Arquier, N., Layalle, S., Bourouis, M., Slaidina, M., Delanoue, R., Bjordal, M., Ohanna, M., Ma, M., Colombani, J., and Leopold, P. 2006. Control of metabolism and growth through insulin-like peptides in Drosophila. *Diabetes* **55 Suppl 2**: S5-8.

Gems, D. and Partridge, L. 2001. Insulin/IGF signalling and ageing: seeing the bigger picture. *Current opinion in genetics & development* **11**(3): 287-292.

Gershman, B., Puig, O., Hang, L., Peitzsch, R.M., Tatar, M., and Garofalo, R.S. 2007. High-resolution dynamics of the transcriptional response to nutrition in Drosophila: a key role for dFOXO. *Physiol Genomics* **29**(1): 24-34.

Giannakou, M.E., Goss, M., Junger, M.A., Hafen, E., Leevers, S.J., and Partridge, L. 2004. Long-lived Drosophila with overexpressed dFOXO in adult fat body. *Science* **305**(5682): 361.

Goberdhan, D.C., Paricio, N., Goodman, E.C., Mlodzik, M., and Wilson, C. 1999. Drosophila tumor suppressor PTEN controls cell size and number by antagonizing the Chico/PI3-kinase signaling pathway. *Genes & development* **13**(24): 3244-3258.

Goberdhan, D.C. and Wilson, C. 2002. Insulin receptor-mediated organ overgrowth in Drosophila is not restricted by body size. *Development genes and evolution* **212**(4): 196-202.

Greenwood, J. and Gautier, J. 2005. From oogenesis through gastrulation: developmental regulation of apoptosis. *Seminars in cell & developmental biology* **16**(2): 215-224.

Huang, H., Muddiman, D.C., and Tindall, D.J. 2004. Androgens negatively regulate forkhead transcription factor FKHR (FOXO1) through a proteolytic mechanism in prostate cancer cells. *The Journal of biological chemistry* **279**(14): 13866-13877.

Hwangbo, D.S., Gershman, B., Tu, M.P., Palmer, M., and Tatar, M. 2004. Drosophila dFOXO controls lifespan and regulates insulin signalling in brain and fat body. *Nature* **429**(6991): 562-566.

Jackson, C. 2006. Diabetes: kicking off the insulin cascade. *Nature* **444**(7121): 833-834.

Johnston, L.A. and Gallant, P. 2002. Control of growth and organ size in Drosophila. *Bioessays* **24**(1): 54-64.

Junger, M.A., Rintelen, F., Stocker, H., Wasserman, J.D., Vegh, M., Radimerski, T., Greenberg, M.E., and Hafen, E. 2003. The Drosophila forkhead transcription factor FOXO mediates the reduction in cell number associated with reduced insulin signaling. *Journal of biology* **2**(3): 20.

Kennedy, S.G., Wagner, A.J., Conzen, S.D., Jordan, J., Bellacosa, A., Tsichlis, P.N., and Hay, N. 1997. The PI 3-kinase/Akt signaling pathway delivers an anti-apoptotic signal. *Genes & development* **11**(6): 701-713.

Kim, A.H., Khursigara, G., Sun, X., Franke, T.F., and Chao, M.V. 2001. Akt phosphorylates and negatively regulates apoptosis signal-regulating kinase 1. *Molecular and cellular biology* **21**(3): 893-901.

Kramer, J.M. 2005. Analysis of the forkhead box subgroup 'O' (FOXO) family of transcription factors and the toxic effects of Gal4 in *Drosophila melanogaster*. In *Biology*, pp. 159. Memorial University of Newfoundland, St. John's.

Kramer, J.M., Davidge, J.T., Lockyer, J.M., and Staveley, B.E. 2003. Expression of Drosophila FOXO regulates growth and can phenocopy starvation. *BMC Dev Biol* **3**: 5.

Lasko, P. 2002. Diabetic flies? Using *Drosophila melanogaster* to understand the causes of monogenic and genetically complex diseases. *Clin Genet* **62**(5): 358-367.

Lee, H.H. and Frasch, M. 2004. Survey of forkhead domain encoding genes in the Drosophila genome: Classification and embryonic expression patterns. *Dev Dyn* **229**(2): 357-366.

Leevers, S.J. 2001. Growth control: invertebrate insulin surprises! *Curr Biol* **11**(6): R209-212.

Manning, B.D. and Cantley, L.C. 2007. AKT/PKB signaling: navigating downstream. *Cell* **129**(7): 1261-1274.

Matsumoto, M., Han, S., Kitamura, T., and Accili, D. 2006. Dual role of transcription factor FoxO1 in controlling hepatic insulin sensitivity and lipid metabolism. *J Clin Invest* **116**(9): 2464-2472.

Miron, M., Verdu, J., Lachance, P.E., Birnbaum, M.J., Lasko, P.F., and Sonenberg, N. 2001. The translational inhibitor 4E-BP is an effector of PI(3)K/Akt signalling and cell growth in Drosophila. *Nature cell biology* **3**(6): 596-601.

Mirth, C.K. and Riddiford, L.M. 2007. Size assessment and growth control: how adult size is determined in insects. *Bioessays* **29**(4): 344-355.

Newsome, T.P., Asling, B., and Dickson, B.J. 2000. Analysis of Drosophila photoreceptor axon guidance in eye-specific mosaics. *Development (Cambridge, England)* **127**(4): 851-860.

Nunez, G. and del Peso, L. 1998. Linking extracellular survival signals and the apoptotic machinery. *Current opinion in neurobiology* **8**(5): 613-618.

Perrimon, N., Lanjuin, A., Arnold, C., and Noll, E. 1996. Zygotic lethal mutations with maternal effect phenotypes in Drosophila melanogaster. II. Loci on the second and third chromosomes identified by P-element-induced mutations. *Genetics* **144**(4): 1681-1692.

Perrot, V. and Rechler, M.M. 2005. The coactivator p300 directly acetylates the forkhead transcription factor Foxo1 and stimulates Foxo1-induced transcription. *Mol Endocrinol* **19**(9): 2283-2298.

Plas, D.R., Talapatra, S., Edinger, A.L., Rathmell, J.C., and Thompson, C.B. 2001. Akt and Bcl-xL promote growth factor-independent survival through distinct effects on mitochondrial physiology. *The Journal of biological chemistry* **276**(15): 12041-12048.

Poltilove, R.M., Jacobs, A.R., Haft, C.R., Xu, P., and Taylor, S.I. 2000. Characterization of Drosophila insulin receptor substrate. *The Journal of biological chemistry* **275**(30): 23346-23354.

Puig, O., Marr, M.T., Ruhf, M.L., and Tjian, R. 2003. Control of cell number by Drosophila FOXO: downstream and feedback regulation of the insulin receptor pathway. *Genes & development* **17**(16): 2006-2020.

Puig, O. and Tjian, R. 2005. Transcriptional feedback control of insulin receptor by dFOXO/FOXO1. *Genes & development* **19**(20): 2435-2446.

Rintelen, F., Stocker, H., Thomas, G., and Hafen, E. 2001. PDK1 regulates growth through Akt and S6K in Drosophila. *Proceedings of the National Academy of Sciences of the United States of America* **98**(26): 15020-15025.

Robertson, H.M., Preston, C.R., Phillis, R.W., Johnson-Schlitz, D.M., Benz, W.K., and Engels, W.R. 1988. A stable genomic source of P element transposase in *Drosophila melanogaster*. *Genetics* **118**(3): 461-470.

Ruggero, D. and Sonenberg, N. 2005. The Akt of translational control. *Oncogene* **24**(50): 7426-7434.

Scanga, S.E., Ruel, L., Binari, R.C., Snow, B., Stambolic, V., Bouchard, D., Peters, M., Calvieri, B., Mak, T.W., Woodgett, J.R., and Manoukian, A.S. 2000. The conserved PI3'K/PTEN/Akt signaling pathway regulates both cell size and survival in Drosophila. *Oncogene* **19**(35): 3971-3977.

Scheid, M.P. 2000. Protein kinase B. *Curr Biol* **10**(10): R358.

Scheid, M.P. and Woodgett, J.R. 2001. PKB/AKT: functional insights from genetic models. *Nature reviews* **2**(10): 760-768.

Slade, J.D. 2005. Control of cell growth through novel alleles of *akt*. In *Biology*, pp. 56. Memorial University of Newfoundland, St. John's.

Slade, J.D., Kramer, J.M. and B. E. Staveley. 2005. A novel luciferase assay for the quantification of insulin signaling in Drosophila. *Drosophila Information Service* **88**: 118-121.

Spradling, A.C., Stern, D., Beaton, A., Rhem, E.J., Laverty, T., Mozden, N., Misra, S., and Rubin, G.M. 1999. The Berkeley Drosophila Genome Project gene disruption project: Single P-element insertions mutating 25% of vital Drosophila genes. *Genetics* **153**(1): 135-177.

Staveley, B.E., Ruel, L., Jin, J., Stambolic, V., Mastronardi, F.G., Heitzler, P., Woodgett, J.R., and Manoukian, A.S. 1998. Genetic analysis of protein kinase B (AKT) in Drosophila. *Curr Biol* **8**(10): 599-602.

Stocker, H. and Hafen, E. 2000. Genetic control of cell size. *Current opinion in genetics & development* **10**(5): 529-535.

Stowers, R.S. and Schwarz, T.L. 1999. A genetic method for generating Drosophila eyes composed exclusively of mitotic clones of a single genotype. *Genetics* **152**(4): 1631-1639.

Tatar, M. 2007. Diet restriction in *Drosophila melanogaster*. Design and analysis. *Interdiscip Top Gerontol* **35**: 115-136.

Tettweiler, G., Miron, M., Jenkins, M., Sonenberg, N., and Lasko, P.F. 2005. Starvation and oxidative stress resistance in Drosophila are mediated through the eIF4E-binding protein, d4E-BP. *Genes & development* **19**(16): 1840-1843.

Theodosiou, N.A. and Xu, T. 1998. Use of FLP/FRT system to study Drosophila development. *Methods (San Diego, Calif* **14**(4): 355-365.

Toker, A. and Newton, A.C. 2000. Akt/protein kinase B is regulated by autophosphorylation at the hypothetical PDK-2 site. *The Journal of biological chemistry* **275**(12): 8271-8274.

Tran, H., Brunet, A., Grenier, J.M., Datta, S.R., Fornace, A.J., Jr., DiStefano, P.S., Chiang, L.W., and Greenberg, M.E. 2002. DNA repair pathway stimulated by the forkhead transcription factor FOXO3a through the Gadd45 protein. *Science* **296**(5567): 530-534.

Twomey, C. and McCarthy, J.V. 2005. Pathways of apoptosis and importance in development. *Journal of cellular and molecular medicine* **9**(2): 345-359.

Van Der Heide, L.P., Hoekman, M.F., and Smidt, M.P. 2004. The ins and outs of FoxO shuttling: mechanisms of FoxO translocation and transcriptional regulation. *The Biochemical journal* **380**(Pt 2): 297-309.

van der Horst, A., Tertoolen, L.G., de Vries-Smits, L.M., Frye, R.A., Medema, R.H., and Burgering, B.M. 2004. FOXO4 is acetylated upon peroxide stress and deacetylated by the longevity protein hSir2(SIRT1). *The Journal of biological chemistry* **279**(28): 28873-28879.

Verdu, J., Buratovich, M.A., Wilder, E.L., and Birnbaum, M.J. 1999. Cell-autonomous regulation of cell and organ growth in Drosophila by Akt/PKB. *Nature cell biology* **1**(8): 500-506.

Vermeulen, K., Van Bockstaele, D.R., and Berneman, Z.N. 2005. Apoptosis: mechanisms and relevance in cancer. *Annals of hematology* **84**(10): 627-639.

Vogt, P.K., Jiang, H., and Aoki, M. 2005. Triple layer control: phosphorylation, acetylation and ubiquitination of FOXO proteins. *Cell Cycle* **4**(7): 908-913.

Whitehead, J.P., Clark, S.F., Urso, B., and James, D.E. 2000. Signalling through the insulin receptor. *Current opinion in cell biology* **12**(2): 222-228.

Wood, K.V., Lam, Y.A., and McElroy, W.D. 1989. Introduction to beetle luciferases and their applications. *Journal of bioluminescence and chemiluminescence* **4**(1): 289-301.

Wu, Q. and Brown, M.R. 2006. Signaling and function of insulin-like peptides in insects. *Annu Rev Entomol* **51**: 1-24.

Yan, N. and Shi, Y. 2005. Mechanisms of apoptosis through structural biology. *Annual review of cell and developmental biology* **21**: 35-56.

Appendix A:

A Novel Luciferase Assay for the Quantification of Insulin Signaling in Drosophila
Slade, J.D., Kramer, J.M. and B.E. Staveley (2005)
Drosophila Information Service **88**: 118-121

A Novel Luciferase Assay for the Quantification of Insulin Signaling in Drosophila

Slade, Jennifer D., Jamie M. Kramer and Brian E. Staveley. Department of Biology, Memorial University of Newfoundland, St. John's, Newfoundland & Labrador, Canada, A1B 3X9; telephone (709) 737-4317; telefax (709) 737-3018; Corresponding author: Dr. Brian E. Staveley; e-mail address: bestave@mun.ca

Introduction

Insulin signaling is implicated in the control of growth and cell survival. One component, the transcription factor FOXO, is activated under low levels of insulin signaling. The shuttling of FOXO between the nucleus and the cytoplasm is mediated by several mechanisms, including its phosphorylation by the akt kinase (van der Heide *et al.*, 2004). Downstream targets of FOXO include genes which influence apoptosis, DNA repair, cell cycle progression, metabolism and oxidative stress resistance (Barthel *et al.*, 2005). Thus, *FOXO* is an important mediator in the control of cellular growth and survival.

Studies in *Drosophila* demonstrate that the evolutionarily conserved insulin signaling pathway is involved in the control of body size and growth, and the reaction to nutritional stress (Kramer *et al.*, 2003; Jünger *et al.*, 2003; Puig *et al.*, 2003). Ectopic expression of *Drosophila FOXO* leads to inhibition of growth and generation of small adults. This occurs via a reduction in cell number and cell size (Kramer *et al.*, 2003). In addition, when there is an excess of *FOXO* activity in larvae, feeding behavior is altered. Newly hatched Drosophila larvae require nutrients in order to increase their body mass via replication of cells in mitotic tissues. In contrast, when larvae are hatched into conditions of amino acid starvation, they live in a state of developmental arrest until nutrients become available (Beadle *et al.*, 1938). Ectopic expression of *FOXO* leads to a phenotype that resembles Drosophila deprived of nutrients (Kramer *et al.*, 2003). As the *Caenorhabiditis elegans* homologue of *FOXO*, *daf16*, is required for the formation of dauer larvae, a unique response to nutritional stress, it has been demonstrated that *Drosophila FOXO* also plays a key role in survival under nutritional stress. Alterations to the insulin signaling pathway and availability of nutrients negatively regulate the activity of *FOXO* (Kramer, Slade and Staveley, submitted). We believe that it is important to understand the fine control mechanisms influencing *FOXO* activity in flies and thus have the basis to comprehend the subtly of its role in human diseases such as diabetes and obesity.

Modern genetic analysis may entail the detection and quantification of gene expression. *In vivo,* this procedure requires the use of a reporter gene that, when introduced into the organism, yields a quantifiable phenotype (Wood, 1995). Transcriptional enhancing elements can be fused to the firefly *luciferase* gene, and then introduced into the fruit fly, *Drosophila melanogaster*. The following describes an assay for the detection of *luciferase* expression from a transgene that responds to alterations in *FOXO* activity.

The *FOXO* recognition element-*luciferase* (*FRE-luc*) transgene

The *FOXO* recognition element-*luciferase* (*FRE-luc*) transgene was created from the 8xFK1tkLuc plasmid construct, which had been demonstrated to respond extremely

well to *FOXO* in cultured cell lines (Biggs *et al.*, 1999). The construct contains eight direct repeats of a *FOXO* recognition element (FRE), and the *luciferase* gene under the control of a herpes simplex virus thymidine kinase minimal promoter. The 8xFK1tkLuc construct was cloned into the *pP{CaSpeR-1}* transformation vector (Figure 1) and then injected into w^{1118} embryos by standard methods. Transgenic flies were selected based on eye colour.

Assay Procedure

Isolation of Drosophila lines containing the FOXO responsive luciferase transgene

Routinely adults are collected in triplicate groups of ten and then flash frozen at -70°C for a minimum of 5 minutes. Flies can be stored at -70°C until ready for protein extraction.

Protein extraction

Protein extraction is performed according to the Promega Luciferase Assay System manual (Promega Corporation, Madison, Wisconsin). Flies are placed in 200 µl of cell culture lysis buffer, and homogenized by grinding in a 1.5 ml microcentrifuge tube. Samples are then subjected to a freeze-thaw cycle three times, that includes flash freezing the samples in ethanol at -70°C, and thawing the samples in a 37°C water bath. The tubes are centrifuged at 10,000 rpm for 10 minutes to remove cellular debris. The supernatant is collected in a fresh tube. The procedure of homogenization, freezing and thawing, centrifugation and collection of supernatant is repeated on the pellet fraction, with the second supernatant pooled with the original.

Determination of Protein Concentration

Protein amounts are quantified using the *DC* Protein Assay kit from Bio-Rad (Bio-Rad Laboratories, Hercules, California). Protein concentrations of extracts were determined against a standard BSA curve and using manufacturer's instructions. Working reagent A, an alkaline copper tartrate solution, and reagent B, a dilute Folin reagent, are required for protein quantification. The proteins and copper react in the alkaline medium, and this leads to the reduction of Folin and colour production. 5 µl of each protein sample is added to wells of a clean, dry microtiter plate. 25 µl of reagent A and 200 µl of reagent B are then added to each protein sample. The plate is gently agitated to mix reagents and samples, and bubbles removed. After 15 minutes, the absorbance of each well is read at 750 nm by a spectrophotometer, such as Spectramax 190 microplate reader (Molecular Devices Corporation, Chicago, Illinois).

Quantification of luciferase expression

To quantify the luciferase activity present in each protein sample, 20 µl of sample plus 100 µl of Steady Glo reagent (Promega Luciferase Assay System) is added to wells in a dark 96-well plate. The plate is then placed into a luminometer, such as a Top Count NXT microplate scintillation and luminescence counter. Amounts of luciferase activity can then be quantified and compared to control samples.

Conclusions

This method represents a novel and accurate way of measuring the activity of endogenous and mutant *FOXO* genes. Indirectly, it can measure the activity of upstream components of the insulin pathway that regulate *FOXO*. For example, as *akt* negatively regulates *FOXO*, an increase in *akt* activity may lead to less *FOXO* activity. In addition, this method can be used to measure the effect of environmental factors, such as age and stress, on the activity of endogenous *FOXO*.

Acknowledgements

This work was funded by grants to BES from the Natural Sciences and Engineering Research Council of Canada (NSERC) Discovery Grant program and The Banting Research Foundation. JDS was partially funded by a Memorial University of Newfoundland School of Graduate Studies Fellowship and a graduate student teaching assistantship from the Department of Biology of Memorial University. JMK was funded by NSERC Post-Graduate Scholarship (Doctoral) award. Many thanks are extended to Dr. W. H. Biggs III for the *luciferase* transgene, and Dr. H. Lipshitz for the w^{1118} line. Further thanks go to Justin N. Moores for his comments on the manuscript.

References

Barthel, A., D. Schmoll, T.G. Unterman, 2005. Trends in Endocrinol. Metab. 16: 183-9.
Beadle, G., E. Tatum, C. Clancy, 1938. Biol. Bull. 75: 447-462.
Biggs, W.H. 3rd, J. Meisenhelder, T. Hunter, W.K. Cavenee, K.C. Arden, 1999. Proc Natl Acad Sci USA 96: 7241-6.
Jünger, M.A., F. Rintelen, H. Stocker, J.D. Wasserman, M. Végh, T. Radimerski, M.E. Greenberg, E. Hafen 2003. J. Biol. 2: 20.
Kramer, J.M., J.T. Davidge, J.M. Lockyer, B.E. Staveley, 2003. BMC Dev. Biol. 3: 5.
Puig, O, M.T. Marr, M.L. Ruhf, R. Tjian, 2003. Genes Dev. 17: 2006–20.
van der Heide, L.P., M.F.M. Hoekman, M.P. Smidt 2004. Biochem. J. 380: 297-309.
Wood, K.V., 1995. Curr. Opin. Biotechnol. 6: 50-8.

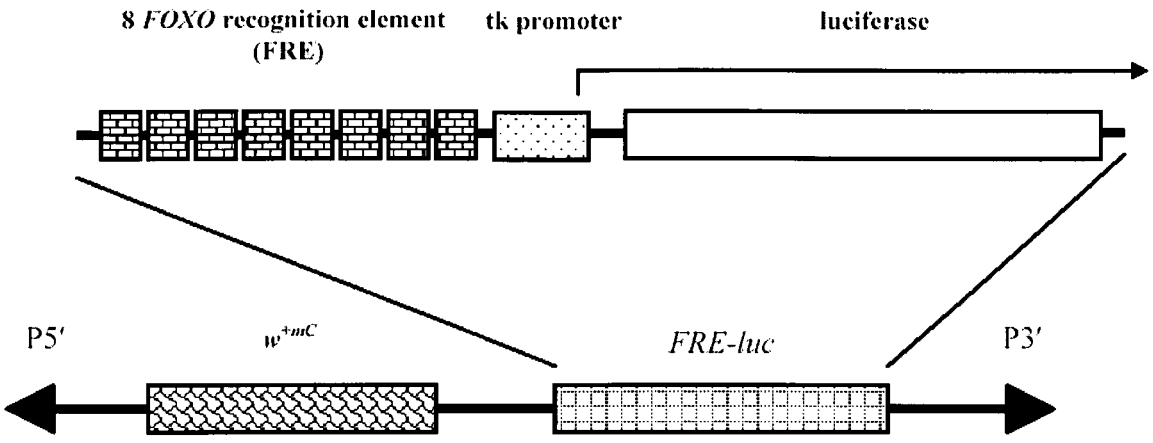

Figure 1: Representation of the *FRE-luc* transgene. Eight direct repeats of the *FOXO* recognition element are located upstream of a minimal herpes simplex thymidine kinase (tk) promoter fused to the *luciferase* gene. Not drawn to scale.

Appendix B:

Comparison of Somatic Clones of the Eye in the Analysis of Cell Growth
Slade, J.D. and B.E. Staveley (2007)
Drosophila Information Service **90:** 151-156

Comparison of Somatic Clones of the Eye in the Analysis of Cell Growth

Slade, Jennifer D. and Brian E. Staveley. Department of Biology, Memorial University of Newfoundland, St. John's, Newfoundland & Labrador, Canada, A1B 3X9; telephone (709) 737-4317; telefax (709) 737-3018; Corresponding author: Dr. Brian E. Staveley; e-mail address: bestave@mun.ca.

Introduction

Cell proliferation and increases in cell size are the processes that contribute to cell growth. Organs or tissues have a tendency to develop within the constraints of a normal final size, and vary from a large number of small cells to a small number of large cells (Day and Lawrence 2000). One important pathway in the control of cellular growth is the insulin receptor signaling pathway which is highly conserved among invertebrates and mammals (Brogiolo *et al.* 2001). When manipulated, several components of this pathway can alter growth rates of *Drosophila melanogaster*. The Drosophila eye normally consists of 700 to 800 ommatidia that develop in a highly regulated manner (Baker 2001) and is ideal for the study of cell growth and cell survival. Mosaic eye clones can be created via the yeast site-specific recombination FLP/FRT system (Theodosiou and Xu 1998), which depends upon the presence of *FRT* sites and expression of the enzyme FLP directed in the developing eye tissue. In the presence of FLP, homologous chromosomes undergo mitotic recombination between the *FRT* sites located on chromosome pairs. Heterozygous parent cells produce homozygous tissue within a heterozygous organism. In this paper, two methods of generating somatic clones of the eye are compared in the study of cell growth.

Drosophila Strains and Culture

Experiments were carried out on standard media containing cornmeal, molasses, yeast, agar and water at 25°C. The control line *w; +/+; P[FRT ;w^{+}]^{2A} P[ry^{+} neo^{R} FRT]^{82B} akt1^{+}* (*w; FRT^{2A} FRT^{82B} akt1^{+}*) was obtained from Dr. Norbert Perrimon, Harvard University (Perrimon *et al.* 1996). The P-element insertion line *akt1^{04226}* was obtained from the Bloomington Drosophila Stock Center. This line contains a P-element inserted within the 5' untranslated region of the *akt1* gene on the third chromosome (Perrimon *et al.* 1996; Spradling *et al.* 1999). The novel derivative of *akt1^{0422}*, *akt^{PR52}*, was generated by imprecise excision. Both *akt1^{04226}* and *akt1^{PR52}* were then recombined with the third chromosome *FRT*'s by standard means, and therefore have the genotype of *w; +/+; P[FRT ;w^{+}]^{2A} P[ry^{+} neo^{R} FRT]^{82B} akt1^{04226}(or ^{PR52})/TM6B* (*w; FRT^{2A} FRT^{82B} akt1^{04226} (or ^{PR52})*). The stocks required for creation of somatic clones of the eye were received from the Bloomington Drosophila Stock Center. The full genotype of Drosophila stock containing *eyeless-FLP* is *y^{d2} w^{1118}; P{ry$^{+t7.2}$=ey-FLP.N}^{2}, P{GMR-lacZ.C(38.1)}^{TPN1}; P{ry$^{+t7.2}$=neoFRT}^{82B}, P{w^{+t*} ry^{+t*}=white-un1}^{90E}, l(3)cl-R3^{1}/TM6B, P{y$^{+t7.7}$ ry $^{+t7.2}$=Car20y}^{TPN1}, Tb^{1}* for method one (Newsome *et al.*, 2000), hereby termed the *ey-FLP* method. The genotype *y w; P{w^{+m}=GAL4-ey.H}$^{3-8}$, P{w^{+mC}=UAS-FLP1.D}^{JD1}; P{ry$^{+t7.2}$=neoFRT}^{82B}, P{w^{+mC}=GMR-hid}^{SS4}, l(3)CL-R^{1}/TM2* (Stowers and

Schwarz, 1999) is the line used for method two, hereby termed the *ey-GAL4/UAS-FLP* method.

Assay Design

Males of *w; FRT^{2A} FRT^{82B} $akt1^{+}$*, *w; FRT^{2A} FRT^{82B} $akt1^{04226}$* and *w; FRT^{2A} FRT^{82B} $akt1^{PR52}$* lines are crossed to females possessing either *eyeless-FLP* or *eyeless-GAL4* and *UAS-FLP* plus the proximal 3R recombination site (*FRT^{82B}*) and a wild-type copy of *akt1*. To obtain the desired individuals, flies are collected upon eclosion based upon phenotypic markers (the absence of *Hu* or *Ubx*). For comparison, homozygous adult males have been analyzed. All collected flies are aged for three to five days, and then flash frozen at –70°C before preparation for Scanning Electron Microscopy (SEM). Preparation included mounting upon aluminum SEM studs, dessication and sputter coating in gold. Three to five images of each genotype are taken by SEM (Hitachi S-570 SEM) at 150X magnification.

Statistical Analysis

Images of each genotype are analyzed using NIH Image J software. Ommatidia and bristles are counted from three images. Ommatidia area is determined by three independent measurements of the area of a cluster of seven ommatidia per picture, for three images. Results are graphed using GraphPad Prism (version 4.02). This program calculates the standard error of the mean to statistically compare the averages of ommatidia number, size and bristle number between genotypes.

Results

Homozygous *akt1* mutant males have phenotypically smaller eyes than wild-type flies (Figure 1). With the *ey-FLP* method, control somatic eye clones developed 711 ± 15 ommatidia, with an area of 223 ± 5 um^2 and 540 ± 14 bristles (Figure 2). The *w; FRT^{2A} FRT^{82B} $akt1^{04226}$* eye was smaller in size compared to the *w; FRT^{2A} FRT^{82B} $akt1^{+}$* control, with 558 ± 14 ommatidia, with an area of 196 ± 4 um^2 and a bristle count of 452 ± 15. This weak allele produced a reduced number of ommatidia and exhibited a small amount of abnormal patterning, as well as misshaped ommatidia, not observed for the control clones. The P element derivative allele *w; FRT^{2A} FRT^{82B} $akt1^{PR52}$* developed smaller and fewer ommatidia than either *w; FRT^{2A} FRT^{82B} $akt1^{+}$* or *w; FRT^{2A} FRT^{82B} $akt1^{04226}$*, with 482 ± 32 ommatidia of an area of 182 ± 3 um^2 and bristle count of 371 ± 33 that had irregular ommatidial pattern. In the *ey-GAL4/UAS-FLP* method, the *w; FRT^{2A} FRT^{82B} $akt1^{+}$* control eye had an average of 704 ± 3 ommatidia with an area of 212 ± 2 um^2 and 563 ± 8 bristles. The *w; FRT^{2A} FRT^{82B} $akt1^{04226}$* eye clones have 508 ± 21 ommatidia of an area of 179 ± 3 um^2 with 377 ± 11 bristles. The derivative *w; FRT^{2A} FRT^{82B} $akt1^{PR52}$* in this method produced 261 ± 8 ommatidia with an area of 149 ± 11 um^2 and 115 ± 11 bristles. All genotypes had some abnormal ommatidial patterning and shape in the *ey-GAL4/UAS-FLP* method. In both methods, the more severe allele, *w; FRT^{2A} FRT^{82B} $akt1^{PR52}$*, was found to be significantly reduced in ommatidia number and size, and in bristle number. However, it is only in the *ey-GAL4/UAS-FLP* method that a significant difference between the control and the weak allele, *w; FRT^{2A} FRT^{82B} $akt1^{04226}$*, was observed.

Discussion

The akt protein kinase is a central component in insulin receptor signaling, and acts through many downstream targets in cell survival, growth, proliferation, metabolism and migration (recently reviewed in Manning and Cantley 2007). Homozygous *akt1*^{1} mutant eyes are small, but co-expression of *akt* in these eyes was able to significantly suppress the reduction in cell size (Staveley *et al.*, 1998; Scanga *et al.*, 2000). Overexpression of *akt* in the developing eye was reported to produce enlarged eyes due to an increase in cell size but not in cell number (Verdu *et al.* 1999). The akt kinase may exert its influence on cell growth through the activation of the target of rapamycin (TOR) complex, and downstream targets S6 kinase 1 (S6K1) and eukaryotic initiation factor 4E binding protein (4EBP) which stimulate the initiation of protein synthesis (Manning and Cantley 2007). In general, the akt kinase can alter cell number through its influence upon cell survival and proliferation, by blocking pro-apoptotic downstream targets BAD (and homologues) and the transcription factor foxo. The akt kinase can influence the overall size of tissues via cell proliferation through downstream target which function within cell cycle regulation. Regardless of the relative contributions of these molecular mechanisms, *akt* activity controls cell growth and survival in the developing Drosophila eye.

Comparison of the Two Methods of Creating Somatic Clones of the Eye

Both methods use *eyeless* enhancers to induce expression of the *FLP recombinase* gene. In the *ey-FLP* method, the *FLP* gene is under the control of four tandem repeats of a specific enhancer from the *eyeless* gene and a basal *hsp70* promoter. This allows for a direct expression of *FLP*. In the *ey-GAL4/UAS-FLP* method, the expression of *FLP* is indirect by the use of the UAS/GAL4 system. The *ey-GAL4* was constructed by cloning a 3.6 kb *Eco*RI fragment containing the eye-specific enhancer of the *eyeless* gene into a vector (Hazelett *et al.* 1998). The expression of *eyeless* begins in the 6 to 23 cell-containing eye disc in embryogenesis and lasts until the last cell divisions required to complete the ~15,000 cell-containing eye disc are carried out during the late third instar (Newsome *et al.* 2000). *FLP* is expressed during this time period and leads to the induction of recombination. There are roughly 10 to 12 rounds of post-embryonic cell divisions necessary to generate the number of cells in the eye disc (Newsome *et al.* 2000). Heterozygous cells can give rise to homozygous cells during subsequent rounds of cell division, and this is increased with the sustained expression of *FLP* and mitotic recombination.

The *ey-FLP* method has been used both with and without the presence of a cell lethal. Without a cell lethal, the *ey-FLP* method results in 20-30% homozygous cells for the mutant allele of interest, and 70-80% of either homozygous or heterozygous wild-type cells (Newsome *et al.* 2000). In the presence of a cell lethal, eye clones produce eyes that consist of 90-100% homozygous cells, although up to 10% of the eye may arise from heterozygous cells (Newsome *et al.* 2000). The cell lethal is therefore able to enhance the generation of clone tissue, and therefore allow for a more complete analysis of homozygous mutant tissue in an otherwise heterozygous animal.

The *ey-GAL4/UAS-FLP* method expresses *FLP* indirectly, so that an amplification of the recombinase is possible. This works through the *eyeless* control sequences enhancing the expression of *GAL4*, and then many copies of the GAL4 protein binding to *UAS* sites to lead to an excess of *FLP* expression. In addition, there is a *GMR-hid*

transgene insertion distal to the *FRT* and wild-type copy of the gene of interest (Stowers and Schwarz 1999). This gene will lead to the death of cells that carry it, including heterozygous cells. The *GMR* promoter leads to the expression of *hid* in late development, during metamorphosis (Stowers and Schwarz 1999). While this is sufficient to remove heterozygous and homozygous wild-type cells, it does not leave sufficient time for the developing eye to compensate. The presence of both *GMR-hid* and a cell lethal allows this method to be effective in eliminating the non-mutant cells, and to produce an almost completely homozygous eye. Calculations determine that the percentage of heterozygous cells will decrease by 0.75 fold to result in the formation of 3 to 5% of the eye (Stowers and Schwarz 1999). This represents a considerably smaller proportion of the eye when compared to the *ey-FLP* method.

Evaluation of Assay

The creation of homozygous clones of the eyes is effective in the study of a mutant phenotype in a heterozygous animal. When the homozygote is developmentally delayed, as is the case with *akt1* mutants (Slade and Staveley unpublished), clones are very informative. In homozygous individuals, a delay in development may allow for compensatory growth that could suppress the homozygous phenotype. The two methods for creating somatic clones of the eye, evaluated here, are more effective in revealing the mutant phenotype when compared to the analysis of the homozygous mutant adults. In the *ey-FLP* method, the *FLP recombinase* gene is expressed directly via the *eyeless* enhancer, and surviving heterozygous cells make up part of the eye. The *ey-GAL4/UAS-FLP* method has the *FLP recombinase* gene expressed in an indirect manner through the UAS-GAL4 system. This allows the amount of the FLP recombinase enzyme to be amplified that may lead to a greater effectiveness in the generation of clones and thus be more sensitive to alterations in growth as observed with *akt1* mutants. In addition, the presence of *GMR-hid* allows for heterozygous cells to be removed from the eye, to produce more clone tissue. These elements suggest that the *ey-GAL4/UAS-FLP* method is a sensitive method for analyzing the growth-dependent mutant phenotype in developmentally delayed adult organisms.

Acknowledgements: This work was funded by grants to BES from the Natural Sciences and Engineering Research Council of Canada (NSERC) Discovery Grant program. JDS was partially funded by a Memorial University of Newfoundland School of Graduate Studies Fellowship and a graduate student teaching assistantship from the Department of Biology of Memorial University. Thanks are extended to Dr. Norbert Perrimon for the *w; +/+; P[FRT ;w^{+}]^{2A} P[ry^{+} neo^{R} FRT]^{82B} (akt1^{+})* line. We thank Jillian Macdonald for a critical review of the manuscript.

References: Baker N.E. 2001, Semin Cell Dev Biol. 12:499-507; Brogiolo W., Stocker H., Ikeya T., Rintelen F., Fernandez R., and Hafen E. 2001, Curr Biol. 11:213-21; Day S.J., and Lawrence, P.A. 2000, Development 127:2977-87; Hazelett D.J., Bourouis M., Walldorf U., and Treisman J.E. 1998, Development 125:3741-51; Manning B.D., and Cantley L.C. 2007, Cell 129:1261-74; Newsome T.P., Asling B., and Dickson B.J. 2000, Development 127:851-60; Perrimon N., Lanjuin A., Arnold C., and Noll E. 1996, Genetics 144:1681-92; Scanga S.E., Ruel L., Binari R.C., Snow B., Stambolic V.,

Bouchard D., Peters M., Calvieri B., Mak T.W., Woodgett J.R., and Manoukian A.S. 2000, Oncogene 19:3971-7; Spradling A.C., Stern D., Beaton A., Rhem E.J., Laverty T., Mozden N., Misra S., and Rubin G.M. 1999, Genetics 153:135-77; Staveley B.E., Ruel L., Jin J., Stambolic V., Mastronardi F.G., Heitzler P., Woodgett J.R., and Manoukian A.S. 1998, Curr Biol. 8:599-602; Stowers R.S., and Schwarz T.L. 1999, Genetics 152:1631-9; Theodosiou N.A., and Xu T. 1998, Methods 14:355-65; Verdu J., Buratovich M.A., Wilder E.L., and Birnbaum M.J. 1999, Nat Cell Biol. 1:500-6.

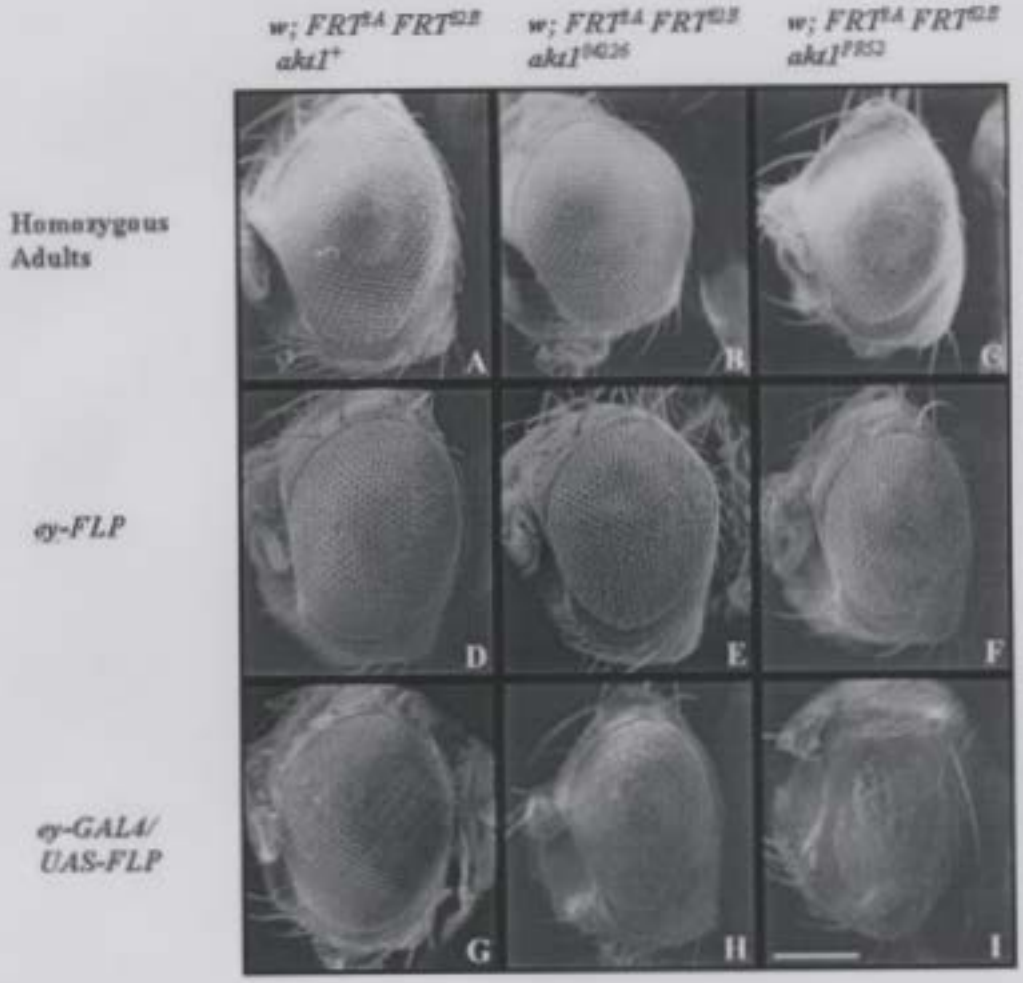

Figure 1: Eyes of *w; FRT^{2A} FRT^{82B} akt1^{+}*, *w; FRT^{2A} FRT^{82B} akt1^{04226}* and *w; FRT^{2A} FRT^{82B} akt1^{PR52}* homozygotes, *ey-FLP*-generated clones, and *ey-GAL4/UAS-FLP*-generated clones. Both methods of creating eye clones counteract the effects of developmental delay, as compared to the homozygous individuals. A-C are from homozygous adult males, D-F are somatic clones of the eye generated by the *ey-FLP* method, and G-I are somatic clones of the eye generated by the *ey-GAL4/UAS-FLP* method. Genotypes are: A, D and G: *w; FRT^{2A} FRT^{82B} akt1^{+}* , B, E, and H: *w; FRT^{2A} FRT^{82B} akt1^{04226}*, C, F, and I: *w; FRT^{2A} FRT^{82B} akt1^{PR52}*. Scale bar represents 160 um.

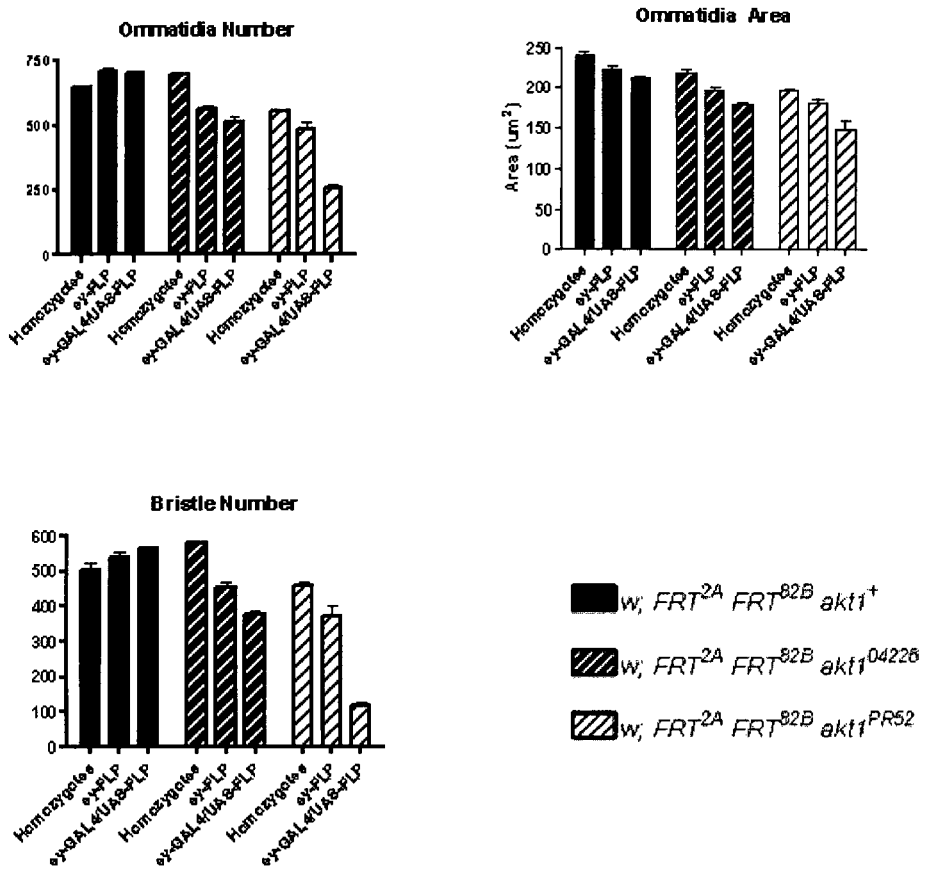

Figure 2: Comparison of ommatidia number, ommatidia size and bristle number of *akt1* mutant homozygotes and somatic eye clones. The control line exhibits a small increase in both ommatidia and bristle number, and a slight decrease in ommatidia area in somatic clones when compared to homozygous individuals. The P-element insertion line *w; FRT^{2A} FRT^{82B} $akt1^{04226}$* has a larger number of smaller ommatidia and bristles compared to the control as a homozygote, but exhibits a decrease in all three phenotypic categories as a clone. The derivative *w; FRT^{2A} FRT^{82B} $akt1^{PR52}$* has fewer ommatidia and bristles, as well as smaller ommatidia, compared to both the control and *w; FRT^{2A} FRT^{82B} $akt1^{04226}$* in all three analyses. This decrease in size and number of cells is the most severe with the *ey-GAL4/UAS-FLP* method.